

# ESTCP Cost and Performance Report

(UX-0035)



## Geonics EM63 Multichannel EM Data Processing Algorithms for Target Location and Ordnance Discrimination

September 2003



ENVIRONMENTAL SECURITY  
TECHNOLOGY CERTIFICATION PROGRAM

U.S. Department of Defense

# COST & PERFORMANCE REPORT

## ESTCP Project: UX-0035

### TABLE OF CONTENTS

		Page
1.0	EXECUTIVE SUMMARY .....	1
2.0	TECHNOLOGY DEVELOPMENT.....	3
2.1	TECHNOLOGY DEVELOPMENT AND APPLICATION.....	3
2.1.1	Blossom Point Configuration and JPG Coil Configuration.....	3
2.1.2	Kaho’olawe Coil Configuration.....	4
2.2	PROCESS DESCRIPTION .....	4
2.3	PREVIOUS TESTING OF THE TECHNOLOGY .....	5
2.4	ADVANTAGES AND LIMITATIONS OF THE TECHNOLOGY.....	5
3.0	DEMONSTRATION DESIGN .....	7
3.1	PERFORMANCE OBJECTIVES .....	7
3.2	SELECTION OF TEST SITE.....	7
3.3	TEST SITE/FACILITY HISTORY/CHARACTERISTICS .....	7
3.3.1	Blossom Point.....	7
3.3.2	Jefferson Proving Ground (JPG V).....	7
3.3.3	Kaho’olawe, Hawaii .....	8
3.4	SAMPLING/MONITORING PROCEDURES .....	9
3.4.1	NAEVA-Geophysical Associates (GPA) Data Quality Control Plans.....	9
3.4.2	Data Acquisition Procedures.....	10
3.4.2.1	General.....	10
3.4.2.2	Blossom Point Data Acquisition Procedures .....	10
3.4.2.3	JPG V Data Acquisition Procedures.....	11
3.4.2.4	Kaho’olawe Data Acquisition Procedures .....	11
3.5	DATA ANALYSIS PROCEDURES.....	11
4.0	PERFORMANCE ASSESSMENT .....	13
4.1	INTRODUCTION .....	13
4.2	BLOSSOM POINT.....	13
4.2.1	Objectives .....	13
4.2.2	Results/Analysis/Conclusion .....	13
4.2.2.1	First Objective: Time Decay Curves.....	13
4.2.2.2	Second Objective: Implementation of EM63 with GPS .....	15
4.2.2.3	Third Objective: Decay Fit and Prioritized Target List.....	20
4.3	JPG V.....	20
4.3.1	Objectives .....	20
4.3.2	Overall Performance Results .....	22
4.3.3	Performance Analysis of Grid 3 .....	24

## TABLE OF CONTENTS (continued)

	<b>Page</b>
4.3.3.1 Multisensor Towed Array Detection System (MTADS) Magnetic Data.....	26
4.4 KAHO'OLAWA .....	26
4.4.1 Objectives .....	26
4.4.2 Results/Analysis/Conclusions.....	26
5.0 COST ASSESSMENT.....	33
5.1 COST REPORTING.....	33
5.1.1 Actual Demonstration Costs .....	33
5.1.2 Costs of Real World Implementation .....	33
5.1.2.1 Pre-Survey Site Visit.....	34
5.1.2.2 Static Bench Testing .....	34
5.1.2.3 Digital Geophysical Mapping .....	35
5.2 COST ANALYSIS.....	35
5.3 COST COMPARISON TO CONVENTIONAL TECHNOLOGY .....	36
6.0 IMPLEMENTATION ISSUES .....	39
6.1 COST OBSERVATIONS.....	39
6.1.1 Project Location .....	39
6.1.2 Project Size .....	39
6.1.3 Terrain Conditions .....	39
6.1.4 Vegetation Conditions .....	39
6.1.5 Geologic Terrain Noise.....	40
6.1.6 Scheduling Requirements .....	40
6.1.7 Potential Cost Reductions/Cost Improvements .....	40
6.2 PERFORMANCE OBSERVATIONS.....	40
6.3 SCALE-UP .....	40
6.4 OTHER SIGNIFICANT OBSERVATIONS.....	41
6.5 LESSONS LEARNED.....	41
6.6 APPROACH TO REGULATORY COMPLIANCE AND ACCEPTANCE.....	41
7.0 REFERENCES .....	43
APPENDIX A POINTS OF CONTACT.....	A-1

## LIST OF FIGURES

		<b>Page</b>
Figure 1.	Configuration of Coils During Blossom Point and JPG V Demonstration .....	4
Figure 2.	Configuration of EM63 During the Kaho’olawe Demonstration .....	5
Figure 3.	Site Map of JPG V Grids .....	8
Figure 4.	Site Map of Kaho’olawe Demonstration Area.....	9
Figure 5.	Check Ashtech GPS Positions, Lane B18-28 .....	9
Figure 6.	Zeroing the EM63 Before Surveying.....	10
Figure 7.	Traversing Kaho’olawe Demo Grid B with the EM63 .....	10
Figure 8.	Decay Curves for a Variety of Inert Ordnance Items Spun at Blossom Point.....	14
Figure 9.	Decay Curves for Lane A, Blossom Point.....	15
Figure 10.	EM63 Gate 10 Test Grid, Blossom Point .....	16
Figure 11.	EM63 Gate 3 Test Grid, Blossom Point .....	17
Figure 12.	EM63 North-South Profile of Lane A, Blossom Point.....	18
Figure 13.	Raw (Unleveled) Profile for Lane Z, Blossom Point.....	19
Figure 14.	Autoleveled Profile for Lane Z, Blossom Point.....	19
Figure 15.	Blossom Point ROC Curve .....	20
Figure 16.	Composite ROC Curves for JPG .....	23
Figure 17.	Contours of Gate 3 Amplitude (mV), Grid 3, JPG .....	24
Figure 18.	Parameter Plots for Decay Curve Shape, Various Ordnance Types.....	25
Figure 19.	Mass Versus Depth Plot for Demo Area A, Kaho’olawe .....	27
Figure 20.	Mass Versus Depth Plot for Demo Area B, Kaho’olawe .....	28
Figure 21.	Mass Versus Depth Plot for Demo Area C, Kaho’olawe .....	28
Figure 22.	ROC Curve for Demo Grid A, Kaho’olawe .....	29
Figure 23.	ROC Curve for Demo Area B, Kaho’olawe .....	29
Figure 24.	ROC Curve for Demo Area C, Kaho’olawe .....	30
Figure 25.	Grid Corner Location Error Histogram for all Demo Areas, Kaho’olawe .....	31
Figure 26.	Emplaced Item Location Error Histogram for Demo Area A, Kaho’olawe .....	31
Figure 27.	Emplaced Item Location Error Histogram for Demo Area B, Kaho’olawe .....	32
Figure 28.	Emplaced Item Location Error Histogram for Demo Area C, Kaho’olawe .....	32

## LIST OF TABLES

		<b>Page</b>
Table 1.	Blossom Point Prioritized Target List EMFIT.....	21
Table 2.	Actual Demonstration Costs .....	33
Table 3.	Presurvey Site Visit Costs.....	34
Table 4.	Static Bench Testing Costs .....	34
Table 5.	Digital Geophysical Mapping Costs .....	35
Table 6.	Cost Comparison to Conventional Technology .....	36

## LIST OF ABBREVIATIONS AND ACRONYMS

---

DAQ	data acquisition
DoD	Department of Defense
EM	electromagnetic
EMI	electromagnetic interference
ERDC	Engineer Research and Development Center
ESTCP	Environmental Security Technology Certification Program
FAC	False Alarm Count
GPA	Geophysical Associate
GPS	Global Positioning System
JPG	Jefferson Proving Ground
JTR	Joint Travel Regulation
MTADS	Multisensor Towed Array Detection System
NAVEODTECHDIV	Natal Explosive Ordnance Disposal Technology Division
NIST	National Institute of Standards and Technology
ng	not to be graded
NRL	Naval Research Laboratory
Pd	percent detected
QA	Quality Assurance
RFP	request for proposal
ROC	receiver operator characteristic
RTK	real-time kinematic
UXO	unexploded ordnance
WES	Waterways Experience Station

## **ACKNOWLEDGEMENTS**

NAEVA and GPA are very grateful for the opportunity to participate in the Kaho'olawe exercise, and for the excellent support provided by ERDC (WES), NAVEODTECHDIV, ESTCP, Parsons, and the Navy. Miro Bosnar and Gil Levy of Geonics Limited were very generous with technical support.

*Technical material contained in this report has been approved for public release.*

*This page left blank intentionally.*

## 1.0 EXECUTIVE SUMMARY

The Department of Defense (DoD) is currently involved in a number of unexploded ordnance (UXO) site remediation efforts where rapid transition of advanced technologies can save substantial sums of money and significantly expedite the transfer of lands for re-use. One of the most prominent of these efforts is the ongoing UXO cleanup of the Kaho'olawe, Hawaii, bombing ranges. The difficulty with this site is that the significant magnetic anomalies from geologic sources and near-surface fragments make traditional magnetometer-based surveys impractical. Standard EM61 metal detection surveys have also performed poorly in these conditions due to the very high magnetic susceptibility response of basalt and basaltic soils. As of March 1, 2000, contractors at Kaho'olawe had detected 12,121 subsurface anomalies, and after digging, they found that only 4% are UXO, 32% are false positives due to geologic variations, and 64% are due to buried metal from both UXO and non-UXO-related materials (Reference 1). The focus of this project was to evaluate the Geonics EM63 multigate time domain metal detector to quantify its detection, discrimination, cost, and production rates. This project was designed to incorporate the lessons learned from previous UXO technology demonstrations and to extend the results of the Jefferson Proving Ground (JPG) Phase IV Demonstrations that were completed during FY 97.

NAEVA Geophysics was contacted by the Environmental Security Technology Certification Program (ESTCP) under Contract Number 200035 to demonstrate detection and discrimination abilities of Geonics' EM63 multichannel (multitime gate) instrument through the development of algorithms and decay curve analysis. The purpose of this advanced technology is to reduce the cost and time spent in UXO remediation. To achieve this goal, the contract was divided into three main tasks. Task One was conducted at NAEVA's office in Charlottesville, Virginia and the Naval Research Laboratory (NRL) Test Field at the Army Research Lab's Blossom Point Research Facility in Maryland to establish an ordnance decay curve analysis database and to develop algorithms for discrimination. Task Two, conducted at JPG in Madison, Indiana, was a government-sponsored blind test to determine the capabilities of the EM63 and other electromagnetic interference (EMI) instruments under a realistic nonmagnetic clutter environment. Task Three was an expansion of JPG conducted on Kaho'olawe, Hawaii, to determine detection and discrimination capabilities under a high magnetic background environment.

The evaluation objectives of the EM63 (and the other systems) were:

1. To evaluate detection and discrimination capabilities under realistic target/geologic clutter/man-made clutter/topography scenarios, while operating as efficiently as possible by minimizing time, manpower, and costs.
2. To evaluate the ability to analyze survey data in a timely manner and provide prioritized "dig lists" with associated confidence levels.
3. To collect manpower, time, productivity, and cost data for all data acquisition and processing tasks.

4. To provide quality, georeferenced data for postdemonstration (off-site) analysis, for development of receiver operator characteristics (ROC) curves, and for use by other government, university, and industry researchers to develop improved analysis technologies.

There were no regulatory issues in connection with NAEVA's ESTCP demonstration performance at Blossom Point, JPG V, or Kaho'olawe. The primary regulatory issue, which will affect the adoption of discrimination technology such as EM63, will be gaining the confidence and approval of federal, state, and local regulators, stakeholders, and users. Acceptance by organizations such as the Army Corps of Engineers and Naval Facilities and Engineering Command will be needed so that future requests for proposals (RFP) will include such innovative technology. This controlled site ESTCP demonstration was the first to employ realistic conditions, which will allow side-by-side comparisons of discrimination performance, production rates, and costs. Acceptance of discrimination technology (that is, not digging part of a prioritized geophysical target list) ultimately requires a cost/risk evaluation by the regulatory agencies.

Overall, the results look extremely promising. In areas of nonmagnetic background, detection is ~92% and discrimination of ordnance from clutter is ~75%. In areas of magnetic background, detection is ~61% and discrimination of ordnance from clutter ~61%. This is an improvement over conventional methods, but many factors influenced these results. For JPG V, nonmagnetic background site, a number of objects were emplaced below the detection threshold. The EM63 is not as effective in detecting small items (20 mm), and the site was not completely cleared before the demonstration began. These factors also influenced Kaho'olawe; in addition, the site was difficult to access.

## **2.0 TECHNOLOGY DEVELOPMENT**

### **2.1 TECHNOLOGY DEVELOPMENT AND APPLICATION**

The EM63 has been modified twice in the last 3 years of this contract by the manufacturer, Geonics Limited, of Toronto, Canada. It generates a pulsed (time domain) primary magnetic field (using a horizontal, multiturn, air cored, 1 m x 1 m transmitter coil 40 cm above the ground surface) that induces Faraday eddy currents and magnetic polarization in nearby metallic and ferromagnetic objects. The decay of the resulting secondary magnetic fields over time is detected in receiver coils 40 cm (bottom coil) and 80 cm above the ground (coaxial with the transmitter coil). The observed decay as a function of time is determined by the character of the target object (size, shape, orientation, and composition). In general, the observed decay is a linear superposition of the axial (longitudinal) and transverse excitation responses of the target object. The transmitter current waveform is bipolar rectangular with 25% duty cycle, 15 amps maximum. The system controller is a PRO4000 field computer (486 AMD processor). The data acquisition (DAQ) dynamic range is 18 bits. Acquisition speed is six records (25 time gates per record) per second. Using the above-mentioned basic configuration, the main receiver, transmitter coils, and data acquisition computer remained the same.

#### **2.1.1 Blossom Point Configuration and JPG Coil Configuration**

The electromagnetic (EM) bottom sensor coil is a circular 50 cm diameter multiturn, air-cored coil, coplanar with the transmitter coil, with 500k Hz bandwidth. The top sensor coil is a 1 m x 1 m square coil 40 cm above the bottom coil and transmitter coil (identical to the EM61 top coil). Twenty to 30 geometrically spaced time gates are measured, covering a range from 180 microseconds to 20 milliseconds (medium base frequency) or 180 microseconds to 7 milliseconds (high base frequency). (See Figure 1.)



**Figure 1. Configuration of Coils During Blossom Point and JPG V Demonstration.**

### **2.1.2 Kaho’olawe Coil Configuration**

The EM bottom receiver coil is a square 0.5 m x 0.5 m multiturn, air-cored coil, coplanar with the 1 m x 1 m transmitter coil. The top receiver coil, also a square 0.5 m x 0.5 m multiturn, air-cored coil, is located 60 cm above the bottom coil. In between (30 cm from the bottom coil) the two 0.5 m x 0.5 m multiturn, air-cored coils, is a third 0.5 m x 0.5 m multiturn, air-cored calibration coil. The second, 1 m x 1 m square coil, is 40 cm above the bottom coil and transmitter coil (identical to the EM61 top coil). However, this coil acts only as a stabilizing coil; it is not a receiver coil as in the previous model used for JPG V. Twenty-six geometrically spaced time gates are measured, covering a range from 180 microseconds to 25 milliseconds. (See Figure 2.)

## **2.2 PROCESS DESCRIPTION**

Refer to Section 3 and Section 4.



**Figure 2. Configuration of EM63 During the Kaho’olawe Demonstration.**

### **2.3 PREVIOUS TESTING OF THE TECHNOLOGY**

NAEVA Geophysics demonstrated the use of the Geonics Protem time domain EM system for UXO discrimination at the Advanced UXO Detection/Discrimination Technology Demonstration at the JPG in 1998. This system was the prototype for the new EM63 multitime gate system that became available late in 1999.

### **2.4 ADVANTAGES AND LIMITATIONS OF THE TECHNOLOGY**

The EM63 multichannel/multitime gate information permits discrimination of various metallic ordnance items from metallic nonordnance items and may also discriminate nonmetallic materials (i.e., basalt and basalt soils) from metallic objects, using the shape of time decay response across the instrument’s 20-30 time gates.

Time decay curve shape analysis permits the recognition of specific ordnance items that have been tested and cataloged in a database. It does not permit generic discrimination of

ordnance from nonordnance by class. Some nonordnance items may, by chance, exhibit decay curves that match certain ordnance items. Therefore, the list of ordnance items to be recognized should be restricted to those actually expected on each particular remediation site. The EM63 technology is still in development and has been modified twice in the last 3 years. The decay curve analysis library must be reestablished and the algorithms modified with each modification.

## **3.0 DEMONSTRATION DESIGN**

### **3.1 PERFORMANCE OBJECTIVES**

NAEVA's primary technical objective was to determine the detection and discrimination capabilities of the EM63 multichannel, time-domain EMI system in nonmagnetic and magnetic clutter environments.

### **3.2 SELECTION OF TEST SITE**

The test site selections were done by ESTCP.

### **3.3 TEST SITE/FACILITY HISTORY/CHARACTERISTICS**

#### **3.3.1 Blossom Point**

NRL Test Field at the Army Research Lab's Blossom Point Facility is a 1,600-acre U.S. Army installation near LaPlata, Maryland, in southern Charles County. The Blossom Point Field Test Facility is an active facility under the U.S. Army Research Laboratory in Adelphi, Maryland. During World War II, Harry Diamond and his team at the National Bureau of Standards (NBS), now named the National Institute of Standards and Technology (NIST) needed open areas where they could test the fuses they were developing. They established test sites at Aberdeen Proving Ground, Maryland; Fort Fisher, North Carolina; and, in early 1943, NBS leased land and established a proving ground for proximity fuses at Blossom Point. By September 1945, 14,000 rocket and mortar rounds had been fired. In 1953, the lease on the property was transferred to the Army, which operated the property as a fast-reaction, low-cost range for experimental work. Firing ranges provided a 2,000-yard maximum range for land impact and a 10,000-yard maximum for water impact. During the Vietnam War, the Army's Harry Diamond Laboratory was very active at the site.

#### **3.3.2 Jefferson Proving Ground (JPG V)**

Inert UXO and natural and manmade clutter items were emplaced at the three controlled grids at JPG for demonstrators to test their detection and discrimination capabilities under realistic conditions and to allow the government to estimate production and cost rates in actual cleanup operations. The three 1-hectare test grids were chosen to provide grids characterized as relatively low, medium, and high magnetic clutter (from geologic sources). Figure 3 shows the locations of these three demonstration grids within the JPG 16-hectare (40 acre) and Waterways Experiment Station (WES) test sites. Grid 1 contains an elongate high magnetic anomaly (+150 nT to -100 nT) and was seeded with the largest concentration of inert UXO targets and clutter items. Grid 2 exhibits a more moderate magnetic response (0 to 35 nT) and irregular topography. Grid 3 contained very low magnetic terrain response and very flat topographic relief. It was seeded with the fewest targets and clutter items. It should be noted that all of these grids are presumably low magnetic relief compared to Hawaiian basaltic terrains, which are normally +/- many *thousands* of nT due to the very high magnetic susceptibilities and magnetic homogeneity of basalt and basaltic soils.

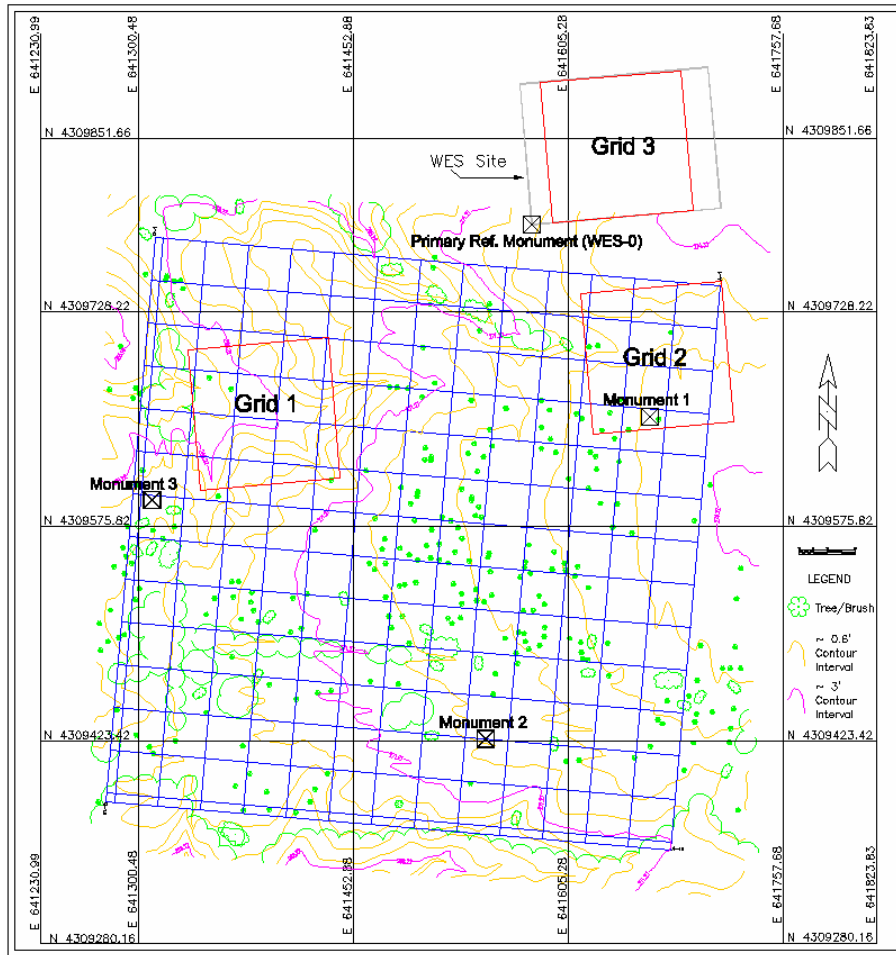


**Figure 3. Site Map of JPG V Grids.**

Plastic flags were placed around the perimeters of the three test grids (oriented to magnetic north), and survey control points were available on or beside all three grids. Twelve inert, cleaned, and degaussed ordnance types, ranging in size from 20 mm to 155 mm, were emplaced on the three test grids, together with representative nonordnance (clutter) items and basaltic samples.

### **3.3.3 Kaho'olawe, Hawaii**

Kaho'olawe Island consists of the summit of a single volcanic dome that reaches a peak elevation of 1,477 ft above mean sea level. The island was used as a weapons range and military training area from 1941 until 1990. In 1993, Title X of the FY 1994 Department of Defense Appropriations Act directed the cleanup of ranges in Kaho'olawe Island. Title X allocated \$400 million for UXO remediation that began in 1993. As of August 2000, only 1,100 acres of the 18,000 acres requiring remediation had been completed. (Reference 2.)

The overall set-up for the exercise is described in the Advanced UXO Detection/Discrimination Technology Demonstration Plan (Reference 5) by the Naval Explosive

Ordnance Disposal Technology Division (NAVEDTECHDIV). Multiple samples of 20 to 30 inert ordnance types and a variety of nonordnance and clutter items were emplaced on three contiguous demonstration grids (A, B, and C), which totaled about 2 hectares. Figure 4 shows the distribution of these demonstration grids (Grid A, composed of four 30 m x 30 m subgrids; Grid B, composed of nine 30 m x 30 m subgrids and three 20 m x 30 m subgrids; and Grid C, composed of six 30 m x 30 m subgrids).

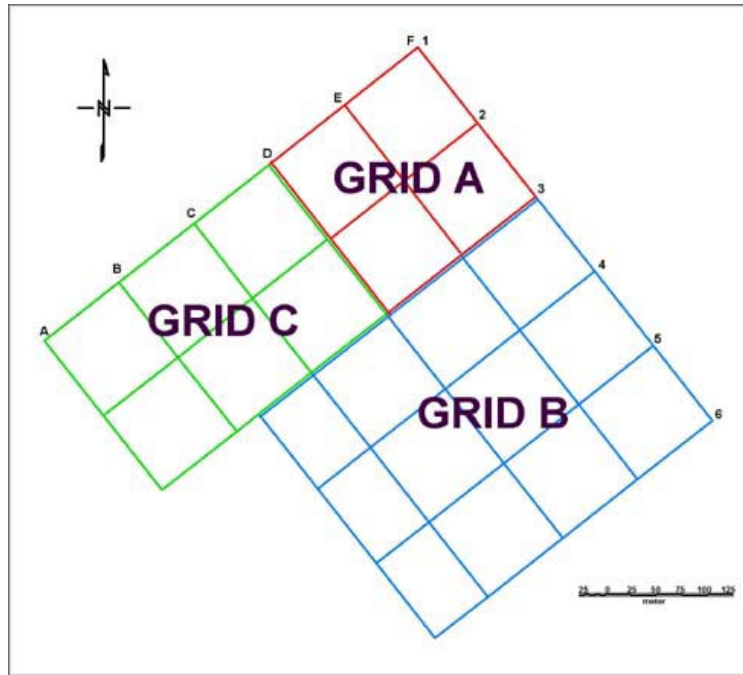


Figure 4. Site Map of Kaho'olawe Demonstration Area.

### 3.4 SAMPLING/MONITORING PROCEDURES

#### 3.4.1 NAEVA-Geophysical Associates (GPA) Data Quality Control Plans

The EM63 was static tested for zero calibration and instrument (plus ambient) noise at the beginning of each survey lane file. The first line was repeated (bidirectional) to verify amplitude and location repeatability. As soon as the file was complete, it was checked for data gaps and/or poor global positioning system (GPS) position recovery, and portions were repeated, if necessary (generally due to poor satellite availability). The repeatability of the first line in each grid lane file (and the amplitude response of the calibration

sphere) was also verified, and terrain noise was inspected. Figure 5 shows GPS position checks

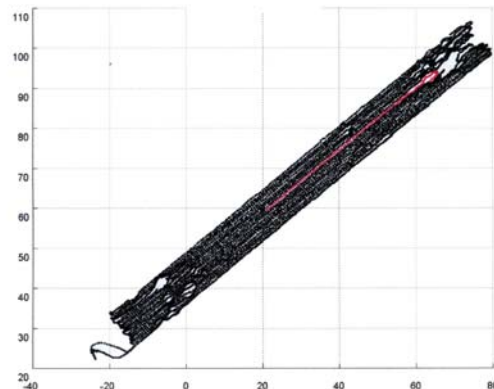


Figure 5. Check Ashtech GPS Positions, Lane B18-28.

for a problematic lane file (lane B18-28, tree at northeast end); black denotes GPS first quality “fix,” while red denotes GPS second quality “float.” Float positions were sometimes, but not always, usable.

### 3.4.2 Data Acquisition Procedures

#### 3.4.2.1 General



**Figure 6. Zeroing the EM63 Before Surveying.**

narrow blocks or lanes approximately 10 m wide over the full northwest-southeast extent of each grid (or contiguous group of grids). This was done due to memory limitations in the EM63 and to avoid longer term zero calibration drift (data acquisition required approximately 30 to 60 minutes per 10 m lane). Figure 7 illustrates surveying with the EM63. Northeast-southwest guide ropes (parallel to prevailing wind) were spaced 2 m apart to ensure straight survey lines with 0.5 m-line spacing.

The EM63 was operated on a nonmetallic test table in static mode at the beginning and end of each lane file to zero the instrument (away from possible background response) before each survey period and to check for calibration drift after each survey period. Figure 6 illustrates EM63 zeroing in air before grid lane surveying.

A standard 3.5 in iron calibration sphere was placed at zero depth just north of the north end of the first survey line in each lane, in order to verify stable amplitude response. The initial line in each lane file was surveyed in southeast and northwest directions to verify data repeatability and satisfactory positional latency (lag) corrections. Data was measured in



**Figure 7. Traversing Kaho’olawe Demo Grid B with the EM63 (ropes at 2 m intervals).**

#### 3.4.2.2 Blossom Point Data Acquisition Procedures

NAEVA made Geonics EM63 field measurements at Blossom Point with new software developed by NAEVA, GPA, and GEONICS that acquired, integrated, and lag-corrected real-time kinematic (RTK) differential GPS for data location over NRL’s original test plot. The test plot, approximately 30 m x 100 m, contained five north-south lanes along which a

variety of target objects were emplaced on 6-foot centers. A small plot, lane Y, with very small ordnance items (50 cal, 20 mm, and 30 mm) was added for NAEVA's exercise. NAEVA also temporarily placed a 3.5-inch diameter iron sphere at zero depth at the north end of each target lane for calibration purposes. In addition, tapes were laid out to help the instrument operator walk straight lines (not necessary with GPS, but helpful to ensure uniform coverage of the surveyed area).

#### **3.4.2.3 JPG V Data Acquisition Procedures**

EM-63 data was acquired on the three 1-hectare test grids, starting with Grid 3, which was conveniently located (near the trailer and a GPS reference monument) and posed the least topographic problems (area was relatively smooth, dry, and level, with few trees and other obstructions). Data was measured in narrow blocks or lanes 10 m wide, over the full 100 m north-south extent of each grid. This was done due to memory limitations in the EM-63, and to avoid longer term zero calibration drift (approximately 40 to 60 minutes per 10 m lane). North-south ropes were spaced 2 m apart to ensure straight survey lines with a 0.5 m line spacing. Each lane was numbered in order from west to east (3-1, 3-2, and so forth). Each raw (binary) lane file contains approximately 2 Mb of data. When necessitated by GPS or other data problems, repeat lane files were measured, and named 3-2b, 3-2c, and so forth. GPS positions were acquired at a rate of 1 per second, and EM-63 readings were collected at a rate of 5 per second, yielding a data density of one reading approximately every 20 cm.

#### **3.4.2.4 Kaho'olawe Data Acquisition Procedures**

In accordance with instructions for Kaho'olawe, the demonstration grids were surveyed in three blocks, which were designated A (the northernmost four 30 m x 30 m grids), B (the 1 hectare grid), and C (the last six 30 m x 30 m grids) (see Figure 4). Data was acquired in northeast-southwest lanes, generally 10 m wide. Each lane was numbered in order from southeast to northwest (A0-10, A10-20, A20-30, etc.). Each raw (binary EM63-GPS composite) lane file contains approximately 1 to 2 Mb of data. When necessitated by GPS or other data problems, repeat lane files were measured and named A10-20b, etc. GPS positions were acquired at a rate of 1 per second, and EM63 readings were collected at a rate of 5 per second, yielding a data density of one reading approximately every 10 to 20 cm.

### **3.5 DATA ANALYSIS PROCEDURES**

The basic EM63 data processing and analysis steps (as practiced at the JPG V demonstration in 2000) are as follows.

1. **GPS checks** – GPS position integration (interpolation, latency corrections).
2. **Autoleveling (all gates)** – To remove decaying background response and calibration drift across all time gates. (This was not possible at Kaho'olawe.)
3. **Visual Inspection (profiles and plan contour maps) and Editing** – To remove bad data points, recognize data gaps, cut outside the grid, and split lines for Geosoft. Repeat DAQ if necessary. Cropping to 0.5 m outside the grid boundaries.

4. **Target Picking** – Selection of all targets over an appropriate amplitude response threshold established by yield curve or data frequency distribution analysis. At Kaho’olawe, it was possible (and necessary) to discriminate basaltic decay response before target picking. Harvest selected decay curves for discrimination analysis.
5. **Comparison of Decay Curves** – From targets and bench calibration tests for expected ordnance items, computation of chi-squared measure of misfit.
6. **Prioritization of target list** – In order of increasing chi-squared misfit.

Autoleveling and target picking are usually the most important and difficult data processing steps. However, at Kaho’olawe, the combination of excessive instrument drift and variable basalt background response made autoleveling impossible. Details of the alternative EM63 data processing and analysis steps as practiced at Kaho’olawe are described below.

In order to remove the effects of the instrumental drift from the data and allow for variable basalt background decay response, a multistep procedure was used. First, the average decay curve of all points in a window (within 30 seconds and 20 m) was subtracted from each decay curve in that window. These adjusted decay curves were then fit with the baseline basalt decay, producing an  $\chi^2$  value, measuring the degree of misfit. The measurements were sorted by  $\chi^2$ , and the lowest 75% were re-averaged, producing a nominal drift baseline without the influence of measured anomalies. This baseline was then subtracted from the data points in the center 10 m of the window to produce the de-drifted data set, the windows were advanced by 10 m, and the procedure was repeated.

This de-drifting produced a data set with both positive and negative basalt response, the former where the basalt level was higher than the local average, the latter where it was lower. Thus, the subsequent fits that include a basalt component allow that component to be either positive or negative.

The de-drifted data was fit with a single basalt component first, producing an  $\chi^2$  map with peaks where the instrument response was non-basalt-like. These peaks were picked with standard Geosoft software, and were then turned into target lists. The discrimination of the targets was performed by simultaneously fitting both a basalt component and components from the ordnance library decay curves to the decay curve of the anomaly. This produced an  $\chi^2$  for each type of ordnance in the library. These  $\chi^2$  values were subtracted from the basalt-only  $\chi^2$ , and these  $\Delta\chi^2$  values (corresponding to log-likelihood ratios in a model comparison test) were used to rank each target.

## **4.0 PERFORMANCE ASSESSMENT**

### **4.1 INTRODUCTION**

NAEVA Geophysics was contacted by ESTCP under Contract Number 200035 to demonstrate detection and discrimination abilities of Geonics EM63 multichannel (multitime gate) instrument through the development of algorithms and decay curve analysis. The purpose of this advanced technology is to reduce the cost and time spent in UXO remediation. To achieve this goal, the above-mentioned contact was divided into three main tasks. Task one, conducted at NAEVA's office in Charlottesville, Virginia, and at the NRL Test Field at the Army Research Lab's Blossom Point Research Facility in Maryland, was to establish an ordnance decay curve analysis database and the development of algorithms for discrimination. The second task, conducted at JPG in Madison, Indiana, was a government-sponsored blind test to determine the capabilities of the EM63 and other EMI instruments under a realistic nonmagnetic clutter environment. Third, an expansion of JPG was conducted on Kaho'olawe, Hawaii, to determine detection and discrimination capabilities under a high magnetic background environment.

### **4.2 BLOSSOM POINT**

The first set of test measurements using Geonics EM63 in conjunction with EMFIT decay-curve analysis software was performed at NRL Test Field at the Army's Research Lab's Blossom Point Research Facility.

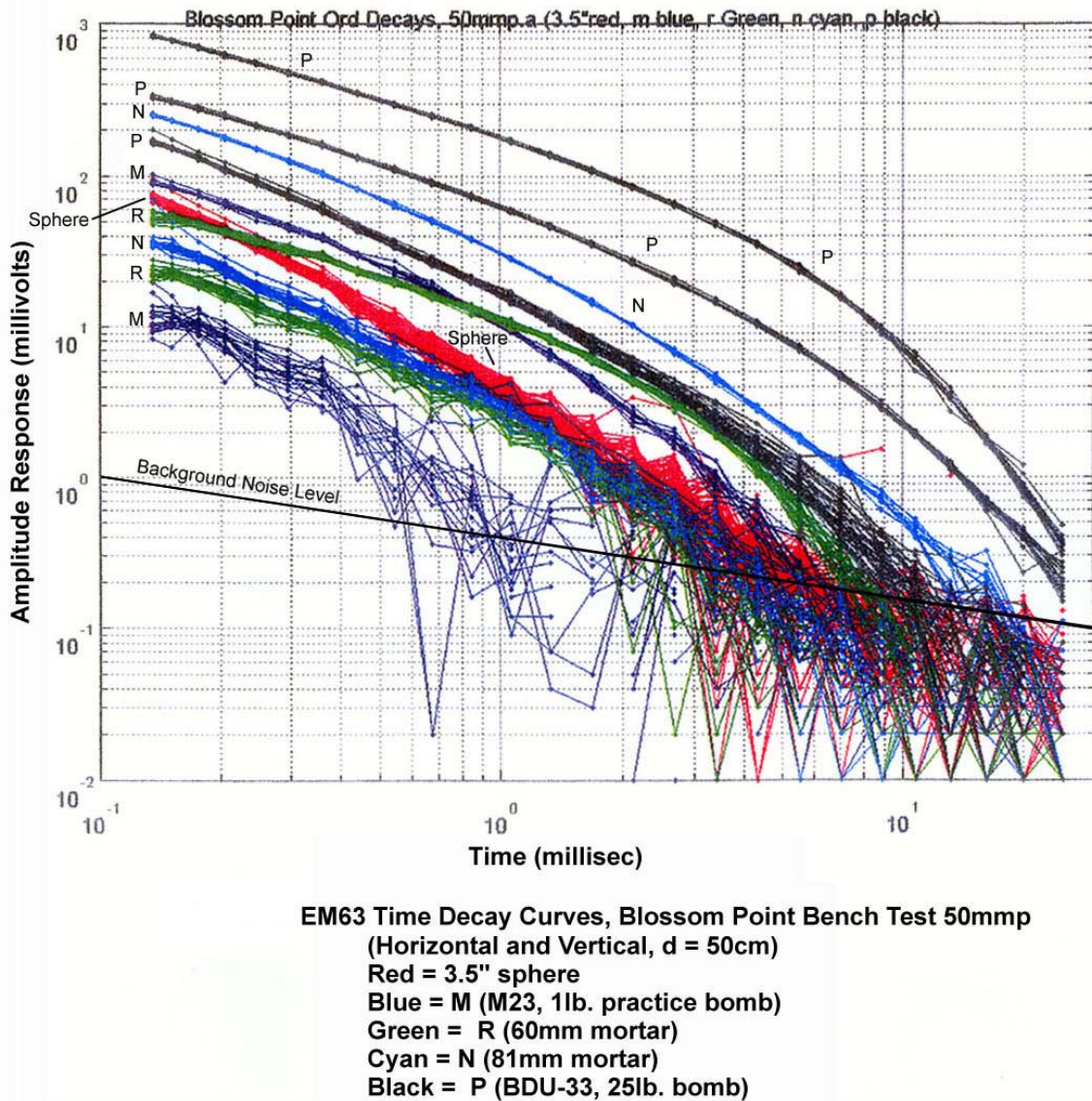
#### **4.2.1 Objectives**

The primary goal of this test was to acquire decay curves from a variety of objects and to verify that the EM63 produced decay curves similar to those observed by NAEVA with the PROTEM receiver at JPG-IV. The second goal was to use an RTK GPS with the EM63 and write software that could integrate the GPS readings with those of the EM63. The third and final goal at Blossom Point was to determine what discrimination of objects could be performed with the EM63 decay curve data, using EMFIT algorithms and software developed by G. H. Ware, H. A. Ware, and W. F. Tompkins of GPA.

#### **4.2.2 Results/Analysis/Conclusion**

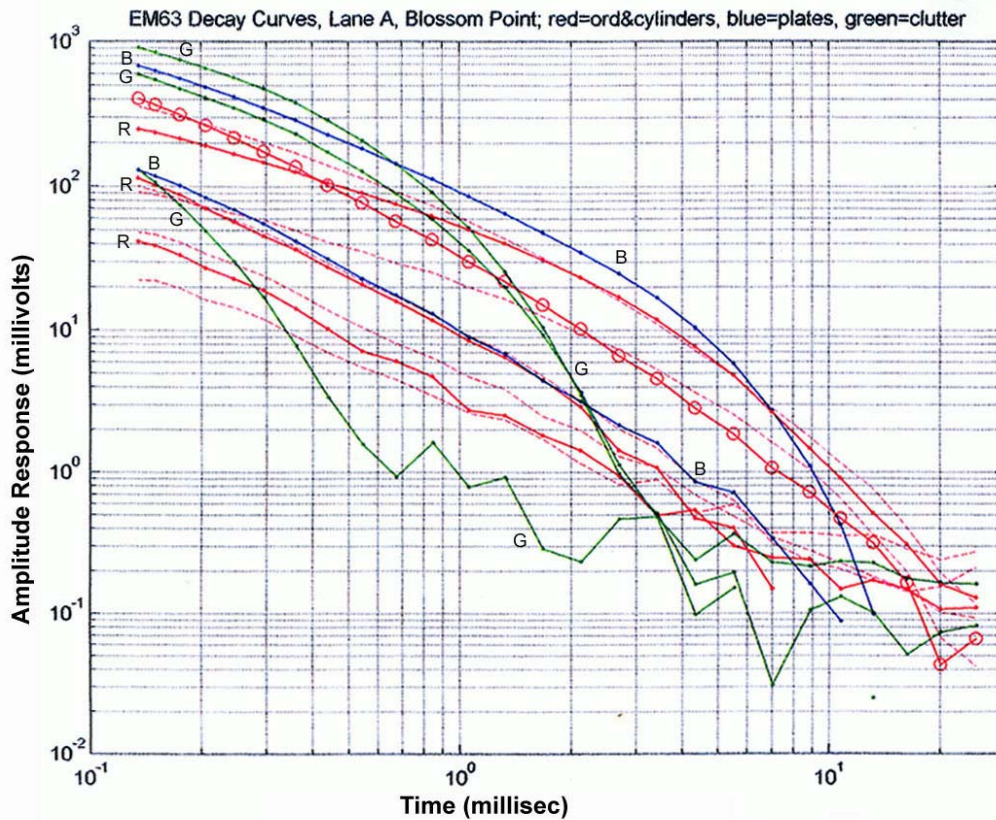
##### **4.2.2.1 First Objective: Time Decay Curves**

Figure 8 shows decay curves from a variety of inert ordnance samples taken at Blossom Point. The sample ordnance and simulant objects were rotated at a depth of 0.5 m under the EM63 to yield the decay curves of each object. Horizontal orientation normally produces a lower amplitude response decay curve and vertical orientation produces higher amplitude response decay curves. Object P (BDU-33) has an unusual response. Instead of producing only one horizontal response, the BDU-33 produces two distinct decay curve responses near the horizontal orientation. For that reason, three black decay curves for item P are represented in Figure 8. The characteristic decay curves agree well with the PROTEM curves generated during JPG-IV. It can be seen from the figure that different types of objects produce distinct curves, which can be used to classify the objects.



**Figure 8. Decay Curves for a Variety of Inert Ordnance Items Spun at Blossom Point.**

Figure 9 shows decay curves from lane A targets. The 16 lb sphere response is red (with small circles). The clutter objects are shown in yellow. EMFIT algorithms and software attempt to prioritize a target list by testing the statistical fit of target decay curves to the known decay curves of ordnance samples (spun under the instrument at all orientations).



EM63 Time Decay Curves, Blossom Point, Lane A Targets  
 Red (R) = ordnance & cylinders (dashed)  
 Red with circles = 16 lb. sphere  
 Blue (B) = plates  
 Green (G) = clutter items

Figure 9. Decay Curves for Lane A, Blossom Point.

#### 4.2.2.2 Second Objective: Implementation of EM63 with GPS

NAEVA made Geonics EM63 field measurements at Blossom Point from May 30 to June 2, 2002. New software developed by NAEVA, GPA, and GEONICS was used to acquire, integrate, and lag-correct RTK differential Trimble GPS for data location. Figures 10 and 11 display the spatial distribution of early gate 3 (better for small objects) and later gate 10 (which approximates the EM61 time gate) from the EM63 data set over NRL's test plot which contained 22 inert ordnance, 22 cylinders, 13 plates, 15 clutter items, and one 16 lb spherical shot-put. NAEVA also temporarily placed a 3.5-inch diameter iron sphere at zero depth at the north end of each target lane, for calibration purposes.

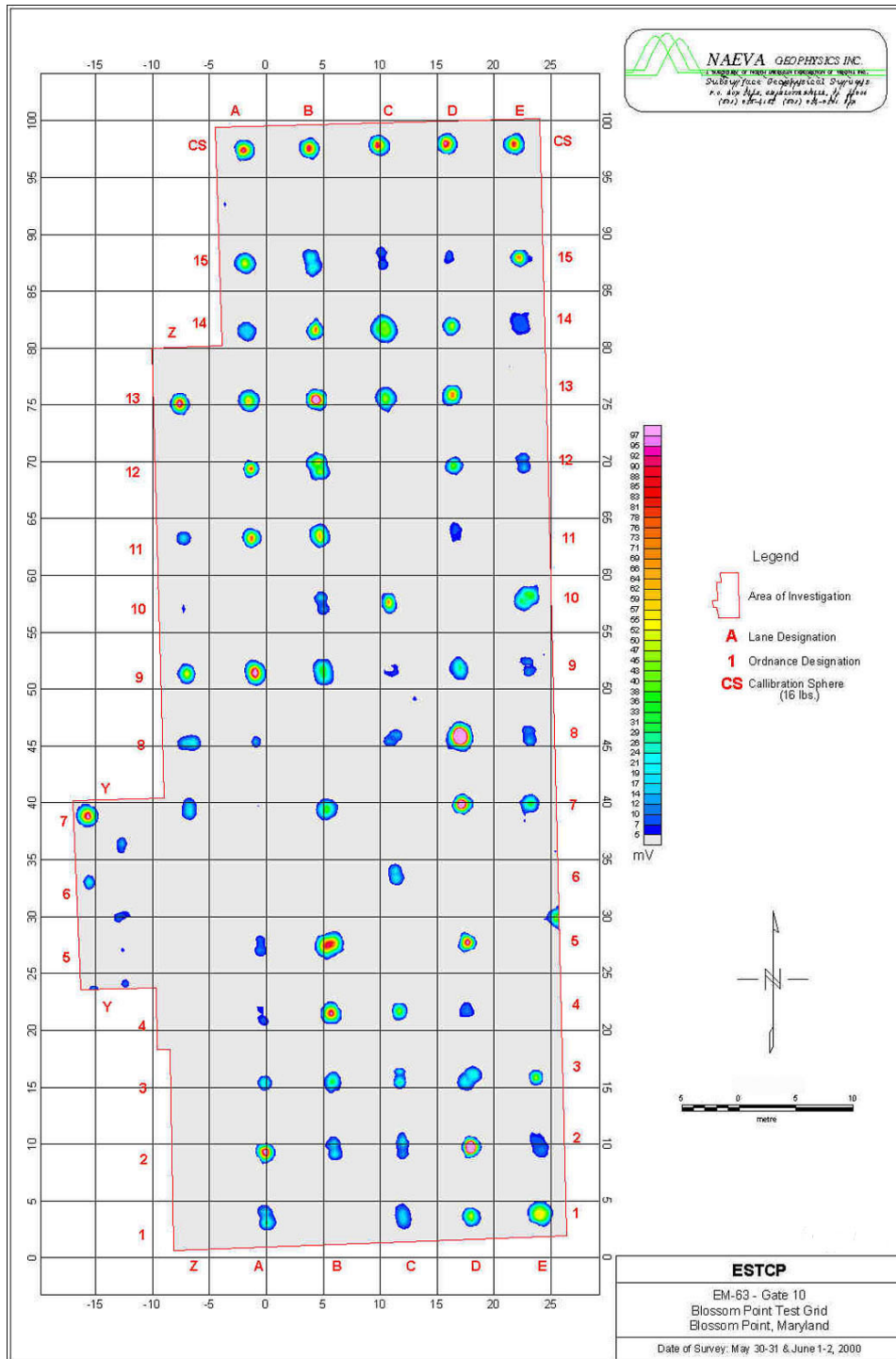
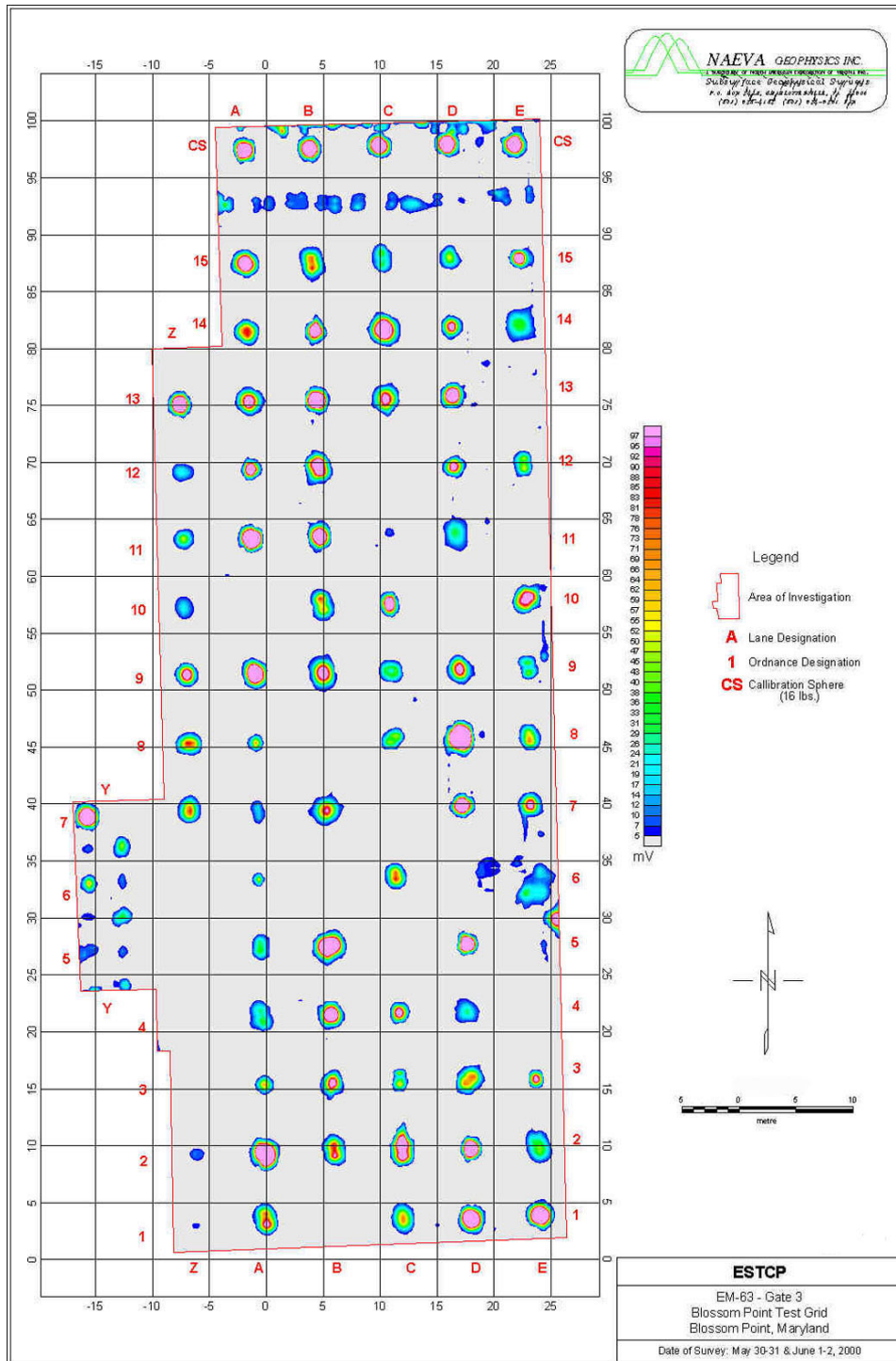


Figure 10. EM36 Gate 10 Test Grid, Blossom Point.

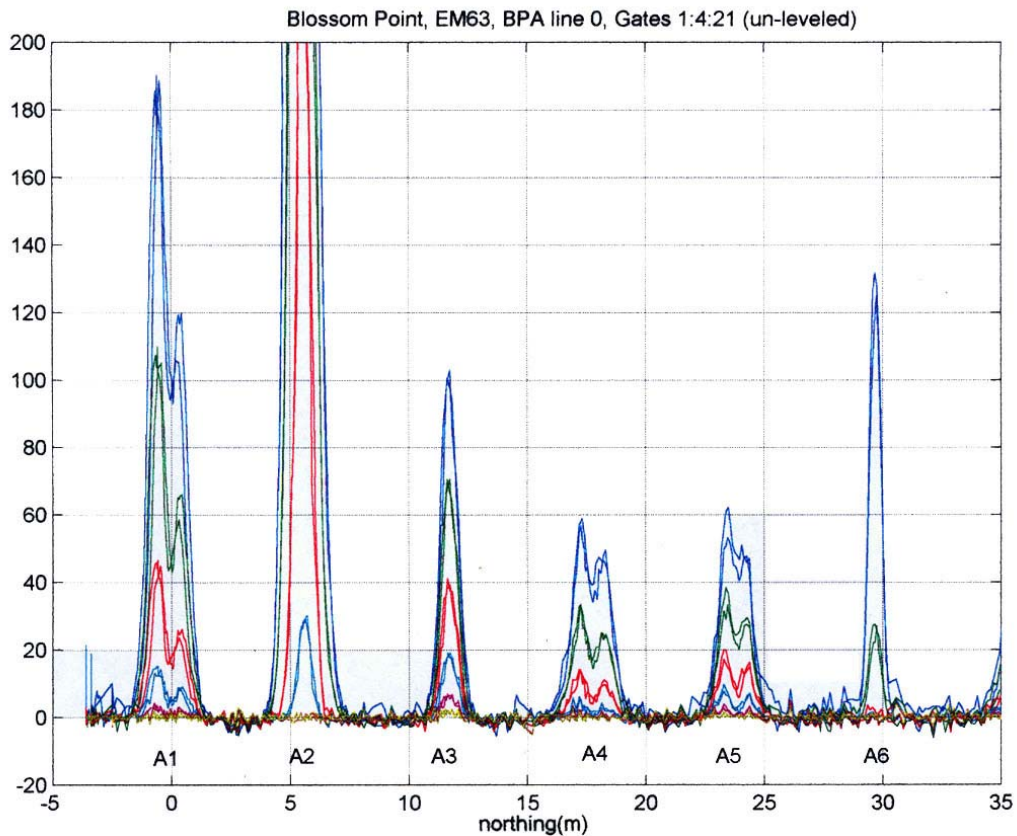


**Figure 11. EM63 Gate 3 Test Grid, Blossom Point.**

It can be seen that all test objects were detected at a 5 mv threshold, at least in the early gate, with the exception of four relatively deep (74–101 cm) 60 mm projectiles at Z3, Z4, Z5, and Z6. The regular shapes of the spatial anomalies indicate that the lagged GPS locations were

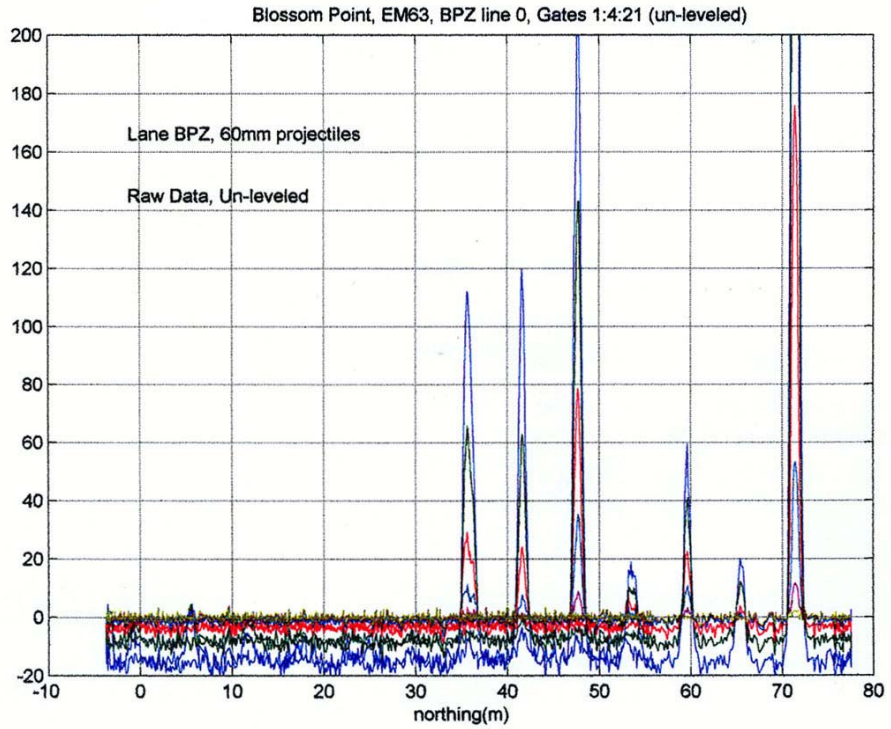
successful. If a comparison of the contour plots and the site layout is made, a few easily explained discrepancies should be noted. As mentioned, a calibration sphere was put approximately 10 m north of each line, resulting in the six uniformly sized anomalies at the top of each target lane. In addition, tapes were laid out to help the instrument operator walk straight lines (not necessary with GPS, but helpful to ensure uniform coverage of the surveyed area). Those tapes had small metallic handles that were placed about 5 m north of each lane. This resulted in slight anomalies in the early gates at those positions.

Figure 12 shows EM63 profiles run north and south along lane A. The alignment of these spatial anomalies also shows that correctly lagged GPS locations were achieved. Note the double peaked response of shallow, horizontal targets.



**Figure 12. EM63 North-South Profile of Lane A, Blossom Point.**

Figure 13 shows a raw (unleveled) EM63 profile along lane Z (the instrument was zeroed before data acquisition, but drifted). Figure 14 shows the same profiles after autoleveling. Clearly, autoleveling is necessary before spatial or decay curve analysis can be done. Figure 14 also shows the essential absence of response to the deep 60 mm targets at Z4, Z5, and Z6. Note the calibration sphere response at the north end of each profile. All of these profiles display gates 1, 5, 9, 13, 17, and 21 only (omitting the rest for clarity).



**Figure 13. Raw (Unleveled) Profile for Lane Z, Blossom Point.**

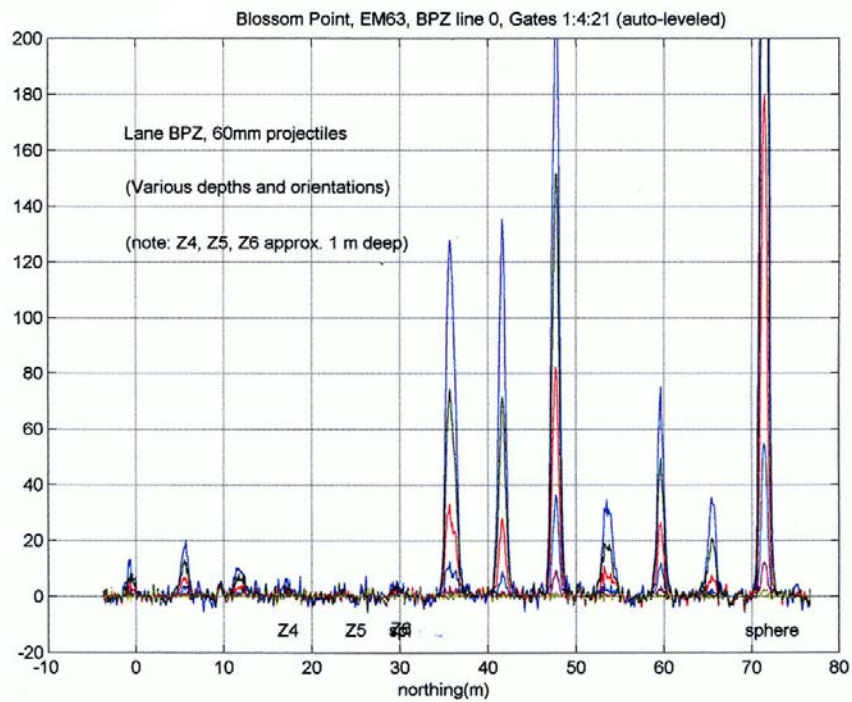


**Figure 14. Autoleveled Profile for Lane Z, Blossom Point.**  
(same profile as above, except autoleveled)

### 4.2.2.3 Third Objective: Decay Fit and Prioritized Target List

Five classes of objects are emplaced in the Blossom Point grid – ordnance, spheres, cylinders, plates, and clutter. It is possible to attempt discrimination between any of these classes. Table 1 displays all the emplaced ordnance and clutter items, arranged in order of statistical goodness of fit to the given ordnance items (NRL code letters M, N, P, and R) by the EMFIT software. M, N, P, and R are identified in Figure 8 and clutter items are number Q1-Q15. Decay curve samples were obtained from bench tests for M, N, P and R. All blossom point ordnance and clutter items (identified by Blossom Point lane and location number) were analyzed.

As already mentioned, items 3-6 in lane Z are relatively deep 60 mm mortars and were not detectable at 5 mV threshold in gates 3 or 10. Item Z3 is barely detectable at a lower threshold (see Figure 14). Decay curves samples from locations of items Z3, Z4, Z5, and Z6 were subjected to chi-squared analysis. Item Z3 was correctly identified as a 60 mm mortar (NRL code R). Locations Z4, Z5, and Z6 were pure noise but gave relatively good chi-squared fits to very low amplitude M or P (NRL code). This problem was recognized and addressed in subsequent analysis and does not occur when only detectable targets are analyzed.

This prioritized list is also displayed as an ROC curve in Figure 15. A satisfactory ROC curve was achieved. Only one clutter item, the horseshoe, appears high in the list (evidently, it has an “ordnance-like” decay curve). The prioritized list hits 100% true positives at 40% false positives (clutter).

## 4.3 JPG V

### 4.3.1 Objectives

The overall technical objective of this demonstration was to evaluate the detection and discrimination capabilities (including production rates and costs) of the Geonics EM63 multitime gate electromagnetic metal detector and associated decay curve, matching algorithms in realistic clutter environments. Three test grids within JPG were prepared to represent a range of conditions in order to identify relative strengths and weaknesses.

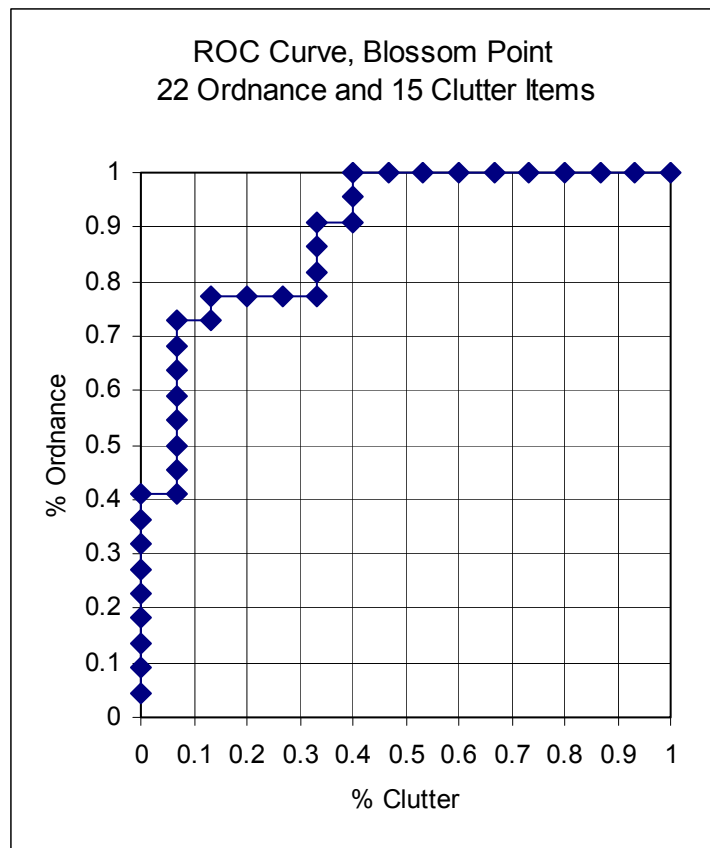


Figure 15. Blossom Point ROC Curve.

**Table 1. Blossom Point Prioritized Target List EMFIT.**

<b>Blossom Point Lane and Location Number</b>	<b>NRL Code</b>	<b>Best-Fit Ordnance Depth (cm) and Type (NRL code)</b>	<b>Chi-Squared Misfit</b>	<b>Nonordnance Items (XXXXX)</b>
Z5	R	50p1	0.78	
Z3	R	50r	1.08	
Z1	R	25r	1.3	
A4	N	50n	1.74	
Z10	R	50n	1.78	
Z6	R	50p	1.8	
B2	M	25m	1.8	
B3	N	50n	1.98	
Z7	R	25r	2.02	
C9	Q12	25m	2.33	XXXXX
Z4	R	50m	2.54	
Z12	R	50m	2.82	
Z8	R	25r	2.92	
Z2	R	50p	3.1	
E2	P	50n	3.45	
B10	M	25m	4.23	
Z11	R	50r	5.34	
E9	Q6	50r	6.49	XXXXX
A1	M	50n	6.52	
B5	Q14	25r	7.93	XXXXX
C10	Q9	25r	8.01	XXXXX
E8	Q15	50n	10.5	XXXXX
B14	M	25m	14.5	
Z9	R	50r	19	
D13	N	50n	30.7	
E1	Q13	50n	36.6	XXXXX
D5	M	25m	67.1	
A13	P	50p	94.3	
C2	Q11	25m	191	XXXXX
D1	Q5	25m	201	XXXXX
C3	Q1	50p	135	XXXXX
D12	Q7	50r	253	XXXXX
E3	Q2	50r	768	XXXXX
A11	Q4	25m	930	XXXXX
D8	Q10	25m	1.17E+03	XXXXX
A6	Q3	25m	2.31E+03	XXXXX
A2	Q8	25m	2.98E+03	XXXXX

The evaluation objectives for the JPG controlled site demonstration of the EM63 were:

- To evaluate detection and discrimination capabilities by means of the three 1-hectare surveys at JPG under realistic target/clutter scenarios and, while operating efficiently, to minimize time and costs.
- To evaluate ability to analyze data on site (NAEVA-GPA did not have on-site processing) and provide prioritized target lists.
- To collect manpower, time, productivity, and cost data for all data acquisition and processing tasks.
- To compare the performance of the Geonics EM63 and other advanced, demonstrated technologies with the baseline magnetic gradiometer and flag technology.
- To provide quality, georeferenced data for postdemonstration (off-site) analysis, for development of ROC curves, and for use by other government, university, and industry researchers to develop improved analysis technologies.

#### **4.3.2 Overall Performance Results**

NAEVA's performance results for Grids 1, 2, and 3 are best summarized by ROC curves generated from the initial (on-site) and subsequent (off-site) prioritized target lists (with and without 20 mm). Figure 16 displays the on-site (with 20 mm) ROC curves and the Percent Detected (Pd) versus False Alarm Count (FAC) points for baseline mag-and-flag. The random (chance) diagonal for Geophex target list is shown as a dashed line in Figure 16. Random diagonals for beginning to the end of NRL's and NAEVA's target list can also be drawn. The high initial slope of the NAEVA ROC curve indicates good detection and discrimination (comparable to NRL, better than Geophex, and considerably better than mag-and-flag across all three grids). The NAEVA EM63 results failed to reach 100% detection at any of the three grids because the gate 3 threshold was set conservatively at 5 mV. The detection would probably have reached 100% at a 4 mV threshold (as shown for Grid 3 in the following self-assessment discussion). NAEVA's Pd performance for all three grids meets Kaho'olawe requirements of 85% with a FAC of approximately 65 for Grid 1, 130 for Grid 2, and 70 for Grid 3.

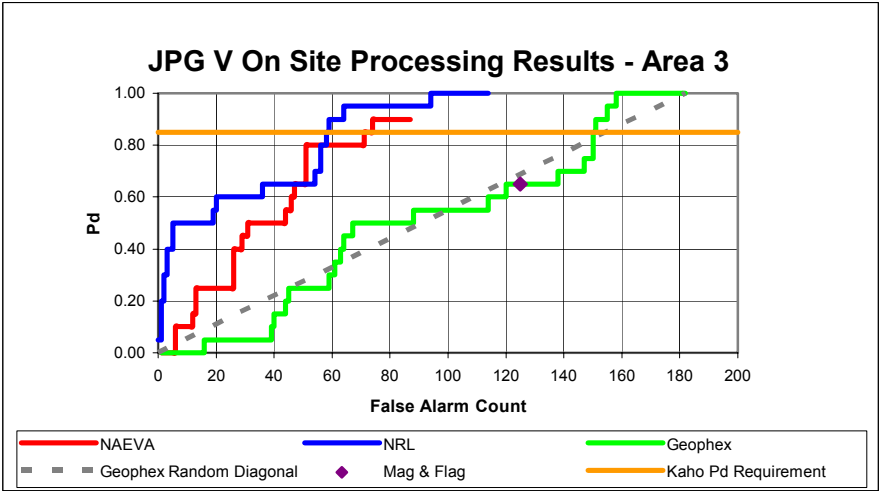
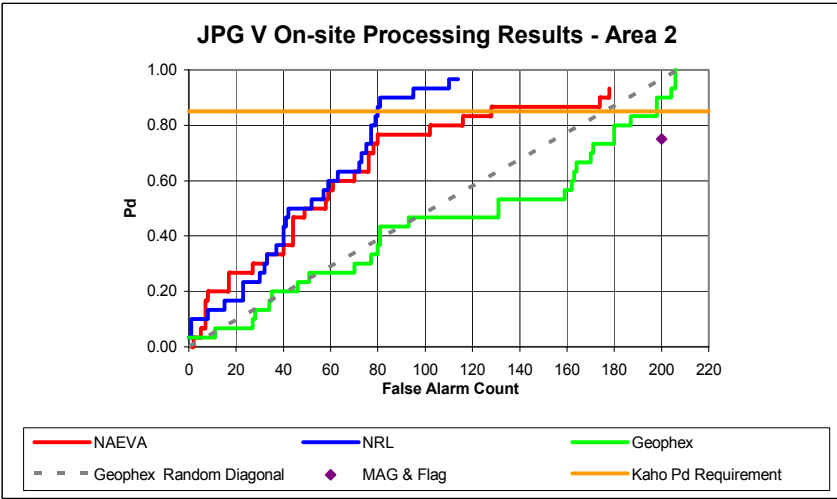
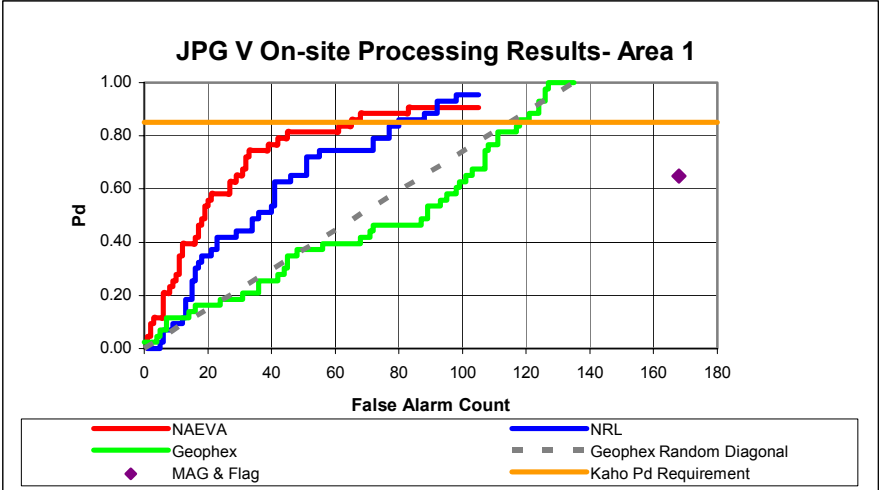


Figure 16. Composite ROC Curves for JPG.

### 4.3.3 Performance Analysis of Grid 3

The JPG Grid 3 truth table has been released, making it possible to evaluate decay curve detection and discrimination as a function of target size, depth, and amplitude response. Results are summarized graphically in Figure 17. All Grid 3 ordnance (red, blue, and yellow triangles) and nonordnance (small uncolored squares) are plotted against mass (x-axis) and depth (y-axis). Two presumed basalt samples (green squares) are shown. Four EM63 gate 3 amplitude contours (threshold 5, 10, 15, and 25 mV) are also shown. These contours were determined by gridding and contouring the gate 3 amplitude response of all detected items that were emplaced. Ordnance that was not detected (outside the 5 mV threshold) is highlighted in blue. Ordnance which was correctly identified is highlighted in yellow. Ordnance which was misidentified by decay curve analysis is highlighted in red. It is interesting that both 57 mm projectiles and almost all of the 60 mm projectiles were misidentified. Most of the 60 mm were misidentified as 81 mm or 152 mm. Parametric plots of decay curve shape were constructed to determine why they were difficult to identify.

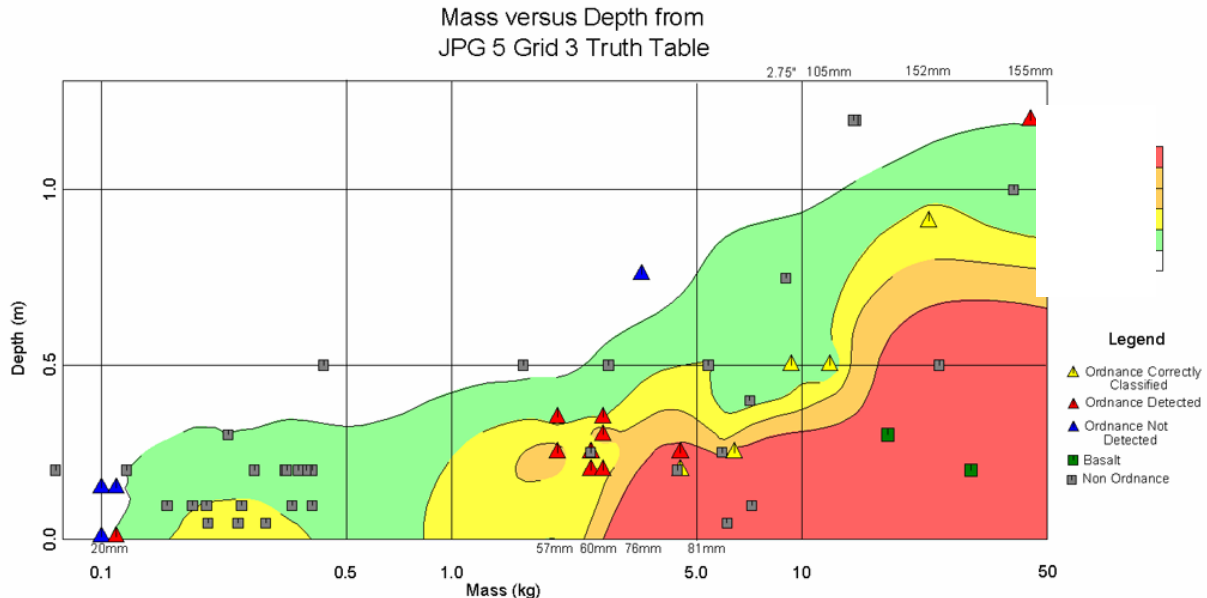


Figure 17. Contours of Gate 3 Amplitude (mV), Grid 3, JPG.

NAEVA Geophysics introduced parametric plots of decay curve shapes in the JPG IV demonstration. Parametric plots display the shape (regardless of depth or amplitude response) in terms of parametric curves based on independent, dimensionless ratio parameters (gate 18/gate 2 is the late decay curve shape and gate 10/gate 2 is the early decay curve shape). If an unknown target plots on one of these parametric curves, it has a similar decay. If parametric curves for two ordnance types overlap, they can not be distinguished by decay shape. Parametric plots or decay curve shape for several of the ordnance samples, shown in Figure 18, reveal that the decay curve shapes for certain sample ordnance types overlap closely. On the other hand, the 9 in long 60 mm projectiles have very distinct decay curves. It is therefore easy to confuse 57 mm and 7 in 60 mm with each other, and also with the 81 mm mortar, 152 mm projectile, and the 3.5 in calibration sphere, especially if the response is noisy (object relatively deep for its size).

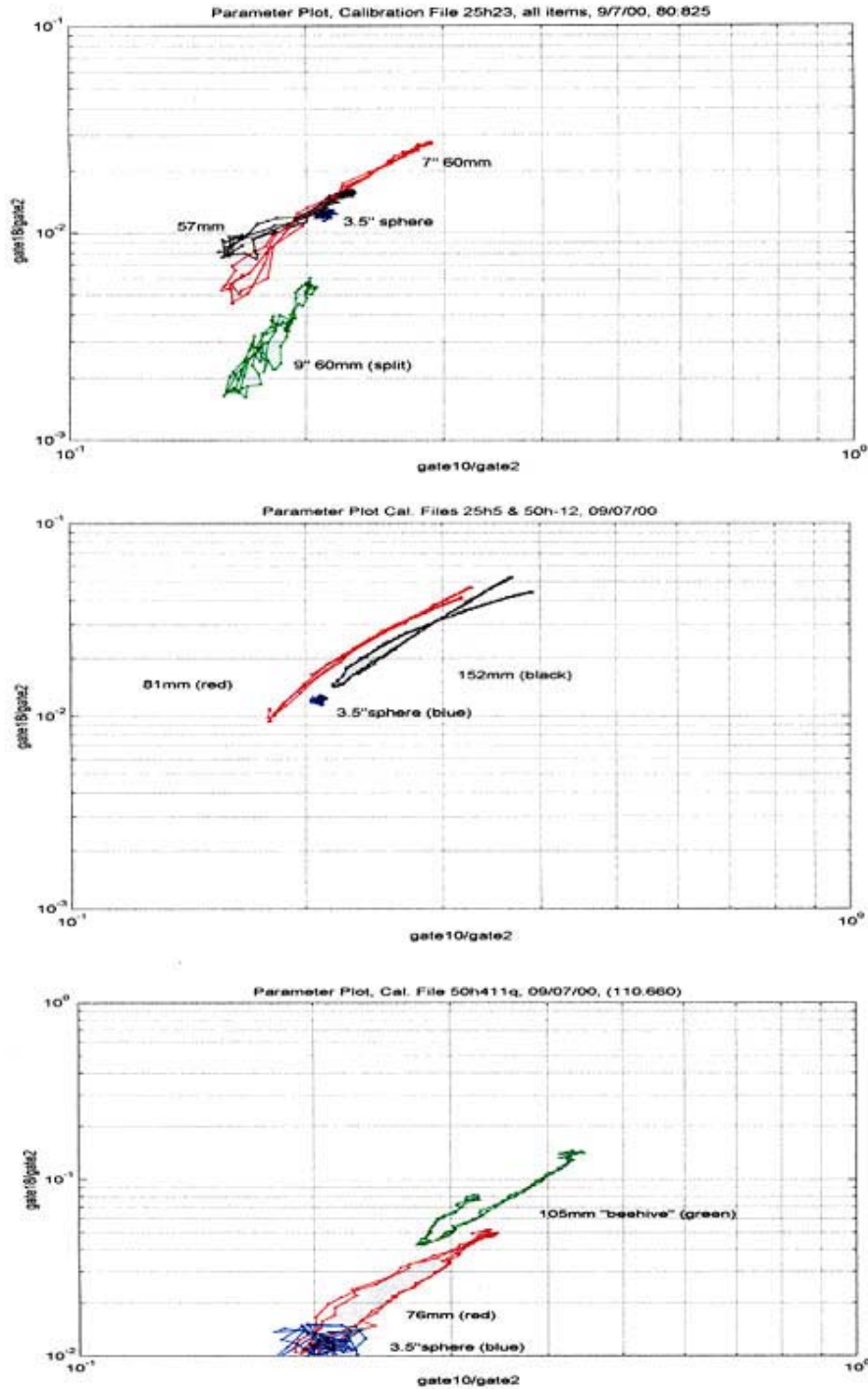


Figure 18. Parameter Plots for Decay Curve Shape, Various Ordnance Types.

Fortunately, this similarity of decay curves for different ordnance does not affect the prioritization of the target list because targets are prioritized if they fit *any* expected ordnance type (in the chi-squared sense).

#### **4.3.3.1 Multisensor Towed Array Detection System (MTADS) Magnetic Data**

MTADS magnetic data was provided after completion of the exercise and submittal of on-site results. The purpose was to use the MTADS data in conjunction with NAEVA's EM63 data for additional postprocessing. Six Grid 3 MTADS magnetic anomalies were selected by visual inspection (with no corresponding EM63 response). Only one of these corresponds to a Grid 3 truth table target (3-110), which is evidently a basalt boulder. The other five correspond to no Grid 3 truth table target; the causes of these anomalies are unknown (but these are almost certainly real objects). The other Grid 3 truth table target that is evidently basalt (3-108) correlates with *no* MTADS or EM response. However, there *is* an MTADS and a weak EM anomaly approximately 2.5 m to the east that is unexplained. Perhaps item 3-108 is mislocated in the Grid 3 truth table.

### **4.4 KAHO'OLAWA**

#### **4.4.1 Objectives**

NAEVA's primary technical objective at the Kaho'olawe Controlled Site Demonstration was to determine the detection and discrimination capabilities of the EM63 multichannel, time-domain EMI system in a high magnetic environment. However, to achieve this main goal, a number of other objectives had to be accomplished during the test, calibration, and revision-optimization period.

- Determine whether the high background response of basaltic materials could be removed (by autoleveling) and/or incorporated into the chi-squared fitting procedures (by use of a characteristic basalt decay vector). To determine this, the following tasks had to be achieved:
  - Evaluation of new compensation coil and other noise reduction measures
  - Measurement and evaluation of the spatially variable background response of basalt and basaltic soils in various locations
- Enlarge the Decay Curve Analysis Library
- Rewrite algorithms for basalt background

#### **4.4.2 Results/Analysis/Conclusions**

Demonstration Grid A (four 30 m x 30 m subgrids) contained 24 emplaced ordnance items, 28 emplaced nonordnance items, and 3 not to be graded (ng) items, according to the final ground truth spread sheet (July 20, 2002). In addition, 18 digs (investigations of unexplained demonstrator targets) were reported, of which 11 were significant (had separate locations, productive of a metal object).

Demonstration Grid B (1 hectare, 12 subgrids) contained 81 emplaced ordnance items, 90 emplaced nonordnance items, and 17 ng, according to the final ground truth spreadsheet (July

20, 2002). In addition, 61 digs (investigations of unexplained demonstrator targets) were reported, of which 34 were significant (had separate locations, productive of a metal object).

Demonstration Grid C (six 30 m x 30 m subgrids) contained 34 emplaced ordnance items, 40 emplaced non-ordnance items, and 11 ng items, according to the final ground truth spreadsheet (July 20, 2002). In addition, 57 digs (investigations of unexplained demonstrator targets) were reported, of which 40 were significant (had separate locations, productive of a metal object).

Our self-evaluation software must input a truth table with classification, mass, and depth information, and a target list. It produces ROC curves, a plan map, a mass-depth diagram (showing detection or not), and a histogram of location errors (up to the detection search radius). Mass information was not provided in the final (May 20, 2002) ground truth spreadsheet. Some masses are estimates; if the mass of an item is not known, it is arbitrarily assigned as 1.0 kg.

The mass-depth diagram (Grid A-Figure 19, Grid B-Figure 20, and Grid C-Figure 21) is probably the most useful display of results because it is possible to draw an approximate limit-of-detection line on the diagram that can be compared to other demonstrators or other sites. The diagram shows the (estimated) masses and depths chosen for emplaced items. It may be seen that the Kaho'olawe detection (using basalt discrimination) approaches JPG detection, which is very satisfying considering the very large basaltic soil response. Detection limit on the mass-depth diagram also provides information needed for remediation planning and quality assurance (QA) of UXO remediation.

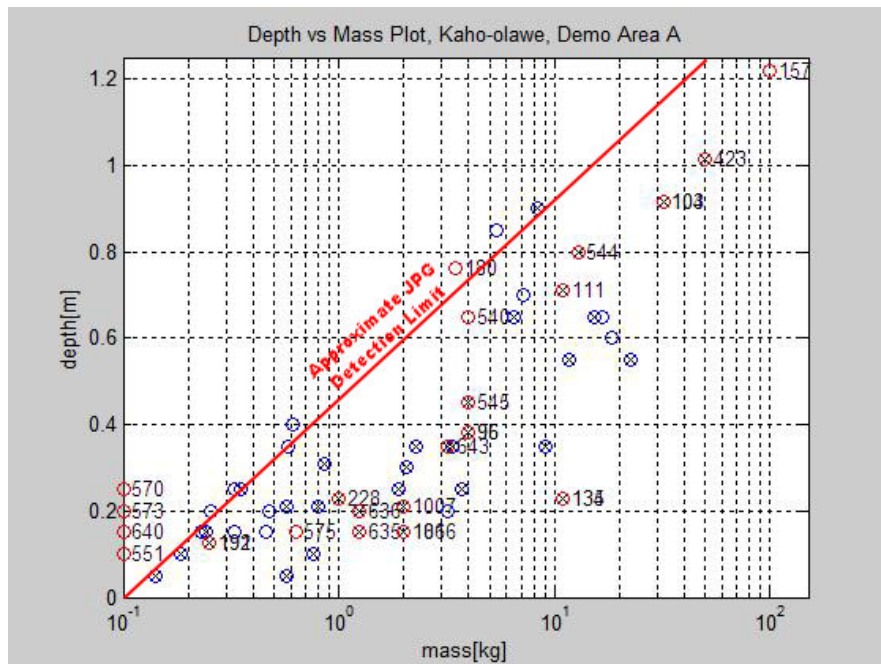


Figure 19. Mass Versus Depth Plot for Demo Area A, Kaho'olawe.

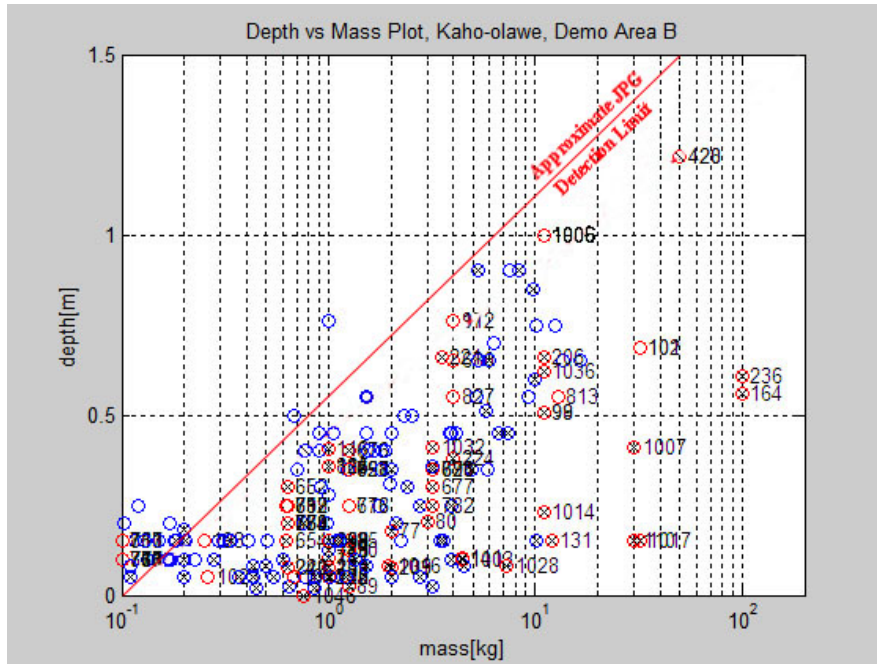


Figure 20. Mass Versus Depth Plot for Demo Area B, Kaho’olawe.

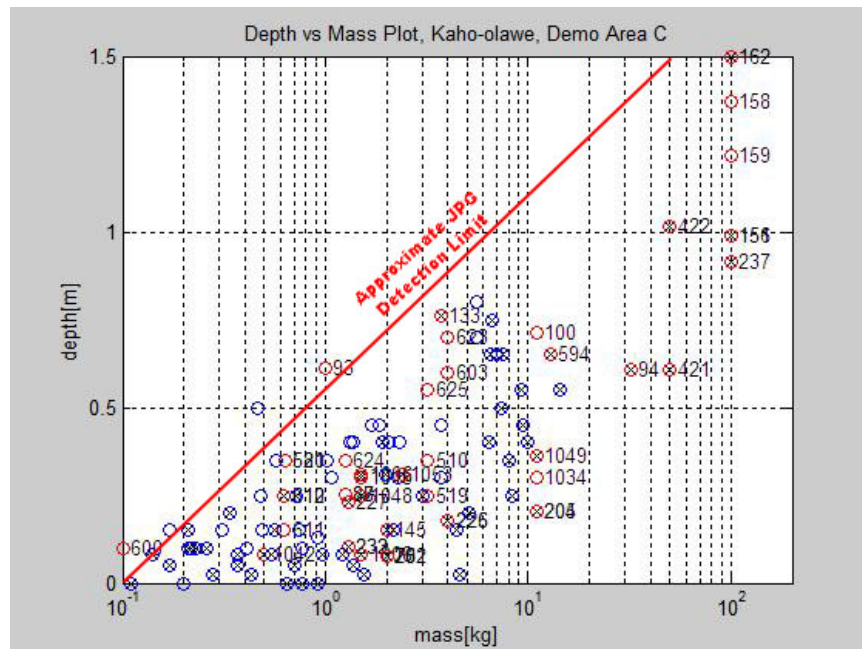
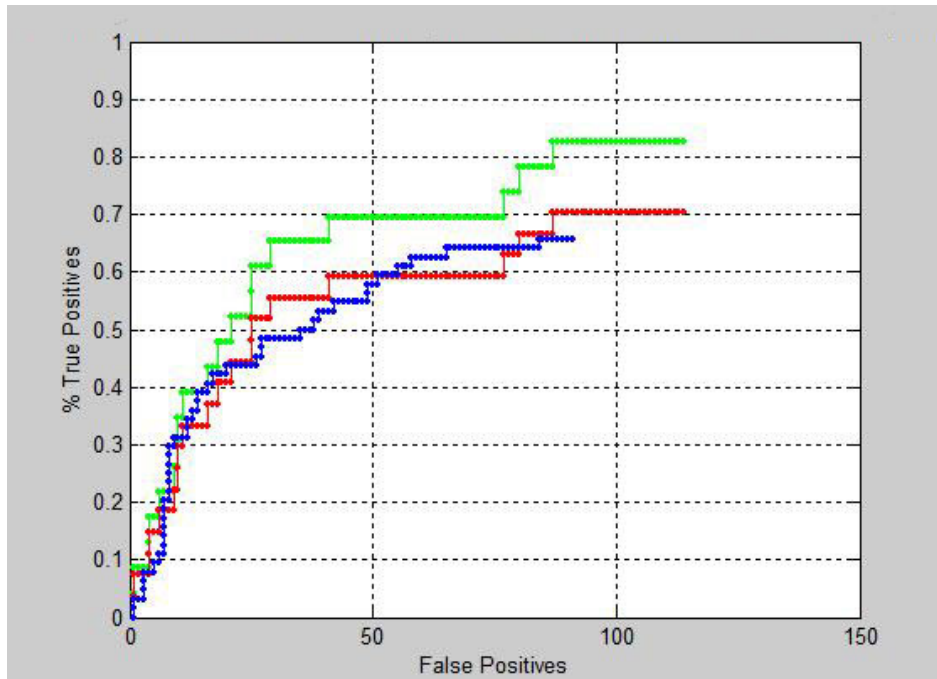
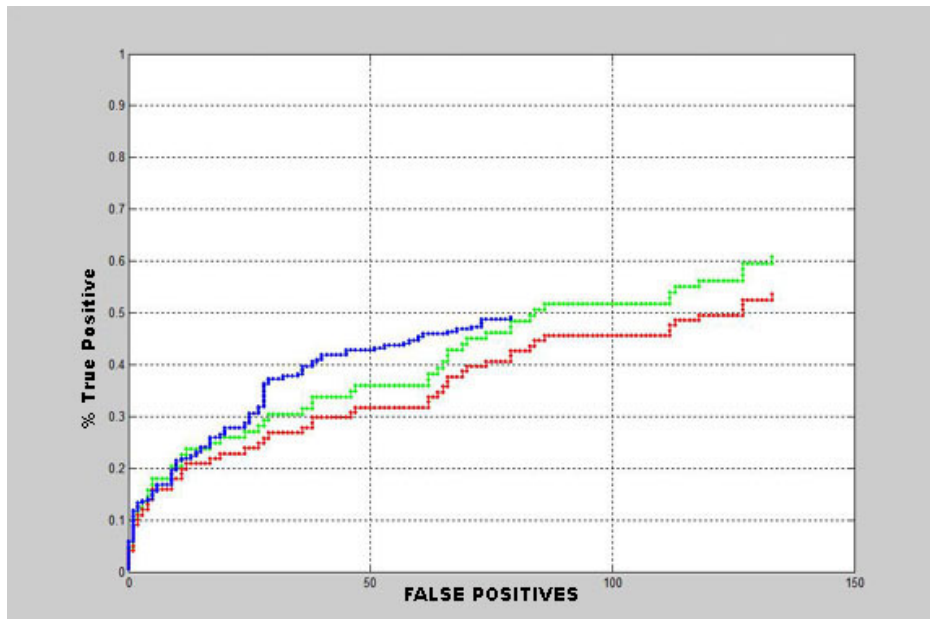


Figure 21. Mass Versus Depth Plot for Demo Area C, Kaho’olawe.

The ROC curves for Demo Areas A, B, and C, respectively (Figure 22, Figure 23, and Figure 24) are dependent on demonstrator merit, site noise, and test item emplacement. Percent true positives depend on the emplacement depth chosen (as a function of item size or mass).



**Figure 22. ROC Curve for Demo Area A, Kaho'olawe.**  
 [Red ROC = all Ordnance, green ROC = Ordnance without 20 mm,  
 blue ROC = all emplaced items (all ordnance, including 20 mm, and nonordnance)]



**Figure 23. ROC Curve for Demo Area B, Kaho'olawe.**  
 [Red ROC = all Ordnance, green ROC = Ordnance without 20 mm,  
 blue ROC = all emplaced items (all ordnance, including 20 mm, and nonordnance)]

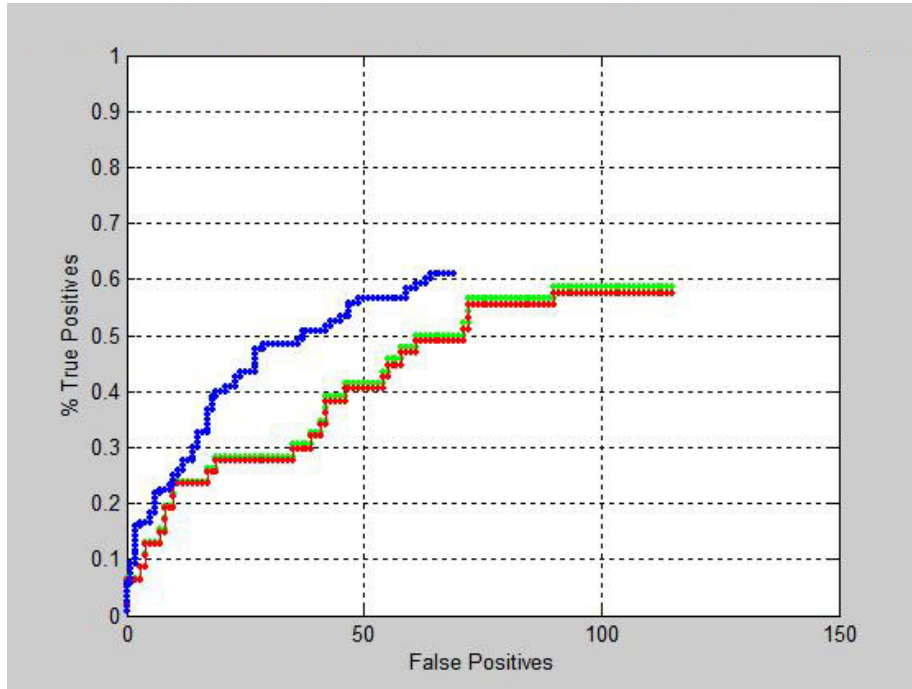


**Figure 24. ROC Curve for Demo Area C, Kaho’olawe.**  
 [Red ROC = all Ordnance, green ROC = Ordnance without 20 mm,  
 blue ROC = all placed items (all ordnance, including 20 mm, and non-ordnance)]

It should be recognized that a large number of detected targets in Demo Grid A (more than 53 of the first 100), Grid B (more than 28 of the first 100), and Grid C (more than 34 of the first 100) prioritized target list do not correspond to any placed or dug items. These are thought to be actual metal objects that were not detected and cleared with the conventional technology. These targets are treated as “false positives” in the ROC curves. For this reason, a more sensitive technology (better detection of metal in basalt) will have a correspondingly worse ROC curve (more false positives).

It appears that NAEVA’s location errors were acceptable based on the location error histogram (Figure 25) of numerous iron rebar rods located on the corners of the 30 m x 30 m subgrids. The mode of these errors is approximately 0.25 m and no mislocations greater than 0.5 m.

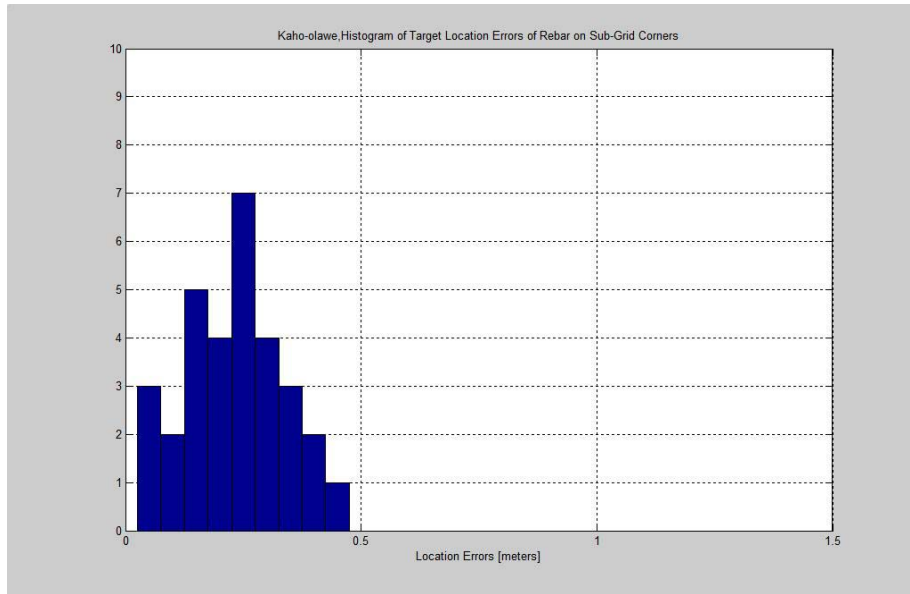


**Figure 25. Grid Corner Location Error Histogram for all Demo Areas, Kaho’olawe** (comparing NAEVA’s target locations to grid corners).

Assuming, based on the acceptable location error histogram explained above, that NAEVA’s locations are correct, Figures 26 (Area A), Figure 27 (Area B), and Figure 28 (Area C) (location error histogram comparing NAEVA targets and the emplaced targets) reveal that a substantial proportion of the emplaced items exhibit location errors between 0.5 m and 1.5 m. These location errors are not due to target location, which is good to 20–40 cm. Of course, these targets will not show up as detected in an ROC curve with a 0.5 m search radius, giving a misleading impression of “% true positives.”

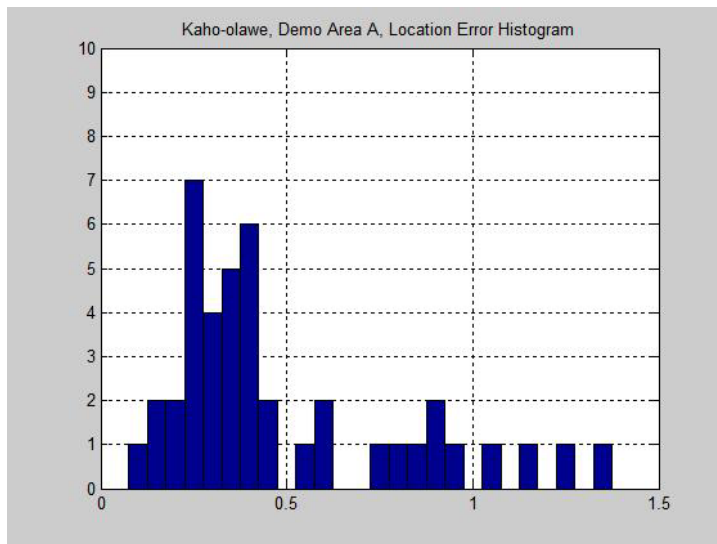


**Figure 26. Emplaced Item Location Error Histogram for Demo Area A, Kaho’olawe** (comparing NAEVA’s target location to the location of the emplaced items).

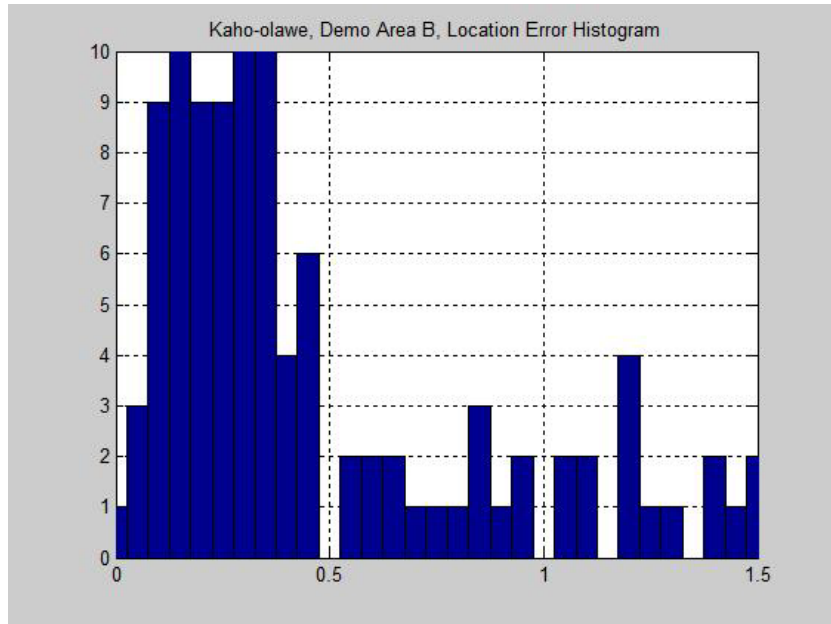


**Figure 27. Emplaced Item Location Error Histogram for Demo Area B, Kaho’olawe** (comparing NAEVA’s target location to the location of the emplaced items).

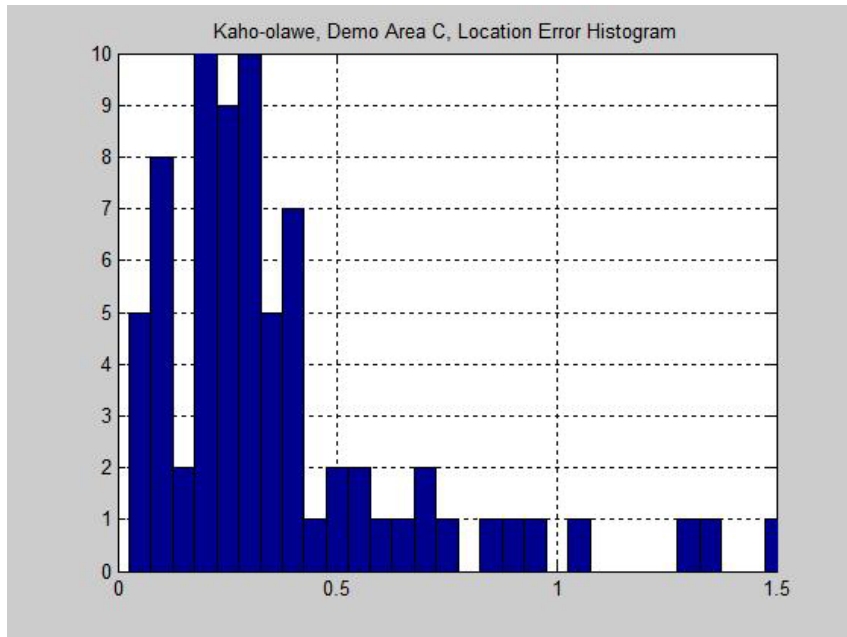


**Figure 28. Emplaced Item Location Error Histogram for Demo Area C, Kaho’olawe** (comparing NAEVA’s target locations to the location of the emplaced items).

## 5.0 COST ASSESSMENT

### 5.1 COST REPORTING

#### 5.1.1 Actual Demonstration Costs

The actual costs incurred for the entire ESTCP Contract Number 200035, EM63 Decay Curve Analysis for UXO Discrimination, was \$361,704. The breakdown of these costs by tasks is outlined in Table 2.

**Table 2. Actual Demonstration Costs.**

<b>Phase I</b>		
Task 1:	Controlled Site Data Acquisition at Blossom Point	\$ 23,520
Task 2:	Data Processing, Algorithm Development, Software Modification	30,800
Task 3:	Controlled Site Demonstration at JPG	57,740
Task 4A:	Final Report Preparation	10,990
Task 4B:	JPG Self-Assessment	11,300
<b>Phase II</b>		
Task 5:	Static Bench Testing	15,150
Task 6:	Initial Kaho'olawe Data Review	16,400
Task 7:	Kaho'olawe Controlled Site Demonstration	94,130
Task 8:	Kaho'olawe Site Data Processing	15,000
Task 9:	Final Report Preparation and IPR Meetings	31,594
Task 10:	Software Preparation	15,480
Task 11:	Kaho'olawe Self-Assessment	39,600
<b>TOTAL</b>		<b>\$361,704</b>

#### 5.1.2 Costs of Real World Implementation

The following table presents estimated expected operational costs for the demonstrated technology when implemented, not including mobilization and demobilization costs and local transportation. A typical project is broken down into three operational phases:

- Presurvey site visit
- Static bench testing
- Digital geophysical mapping
  - Data acquisition
  - Data processing for detection and discrimination

Costs are calculated based on an average daily rate and increase or decrease depending on the size and duration of any specific project.

### 5.1.2.1 Pre-Survey Site Visit

**Table 3. Presurvey Site Visit Costs.**

<b>Item</b>	<b>Cost</b>
<b>Data Acquisition</b>	
Labor	\$1,350
EM63 Equipment	\$ 350
GPS	\$ 250
Per Diem	\$ 240
Materials	\$ 100
<b>Data Processing</b>	
Labor	\$1,040
Software	\$ 100
Materials	\$ 40
<b>Data Presentation</b>	
Labor	\$ 130
Materials	\$ 10
<b>TOTAL (Daily Rate)</b>	<b>\$3,610</b>

It is estimated that a typical project may require a presurvey site visit of 5 days.

### 5.1.2.2 Static Bench Testing

**Table 4. Static Bench Testing Costs.**

<b>Item</b>	<b>Cost</b>
<b>Data Acquisition</b>	
Labor	\$1,350
EM63 Equipment	\$ 350
Materials	\$ 100
<b>Data Processing</b>	
Labor	\$1,040
Software	\$ 100
Materials	\$ 40
<b>Data Presentation</b>	
Labor	\$ 130
Materials	\$ 10
<b>TOTAL (Daily Rate)</b>	<b>\$3,120</b>

It is estimated that a typical project may require static bench testing of the anticipated ordnance items for about 5 days.

### 5.1.2.3 Digital Geophysical Mapping

**Table 5. Digital Geophysical Mapping Costs.**

<b>Item</b>	<b>Cost</b>
<b>Data Acquisition</b>	
Labor	\$1,350
EM63 Equipment	\$ 350
GPS	\$ 250
Per Diem	\$ 240
Materials	\$ 100
<b>Data Processing</b>	
Labor	\$1,040
Software	\$ 100
Materials	\$ 40
<b>Data Presentation</b>	
Labor	\$ 130
Materials	\$ 10
<b>TOTAL (Daily Rate)</b>	<b>\$3,610</b>

It is estimated that a two-person field crew can collect approximately ½ to 1½ acres of survey data per day, depending on field conditions.

## 5.2 COST ANALYSIS

The following comments are offered to support the daily unit cost per item presented in Tables 3, 4, and 5.

- Labor (Data Acquisition): This rate reflects average state-of-the-industry costs for a two-person geophysical field team for a 10-hour workday.
- EM63: This reflects a typical daily use fee a geophysical subcontractor would charge for use of an EM63 instrument in the field. Such a fee would include all repair and maintenance costs, as well as equipment replacement, when the instrument becomes obsolete or unreliable.
- GPS: This rate reflects a typical daily use fee that a geophysical subcontractor would charge for use of a GPS system (rover and base station) in the field, and the software necessary to integrate the GPS data with the EM63 geophysical data. Such a fee would include all repair and maintenance costs, as well as equipment replacement, when the instrument becomes obsolete or unreliable.
- Per Diem: This rate is presented as an average per diem rate for an average project. Actual per diem rates would be those presented in the government joint travel regulations (JTR).
- Materials: An average cost of materials is calculated based on \$10.00 per field crew labor hour and \$5.00 per labor hour of data processing and data presentation.

- Labor (Data Processing): This rate reflects average state-of-the-industry costs for 16 hours of data processing per field day of data acquisition.
- Software: This rate reflects a suggested daily fee for lease of the EM63 data processing software for detection and discrimination, per field team.
- Labor (Data Presentation): This rate reflects average state-of-the-industry costs for 2 hours of data presentation per field day of data acquisition.

### 5.3 COST COMPARISON TO CONVENTIONAL TECHNOLOGY

Table 6 presents a daily cost comparison of the demonstrated EM63 technology to conventional technology.

**Table 6. Cost Comparison to Conventional Technology.**

Item	EM63	EM61	Difference
<b>Data Acquisition</b>			
Labor	\$1,350	\$1,350	\$ 0
EM63 Equipment	\$ 350	\$ 250	\$ 100
GPS	\$ 250	\$ 250	\$ 0
Per Diem	\$ 240	\$ 240	\$ 0
Materials	\$ 100	\$ 100	\$ 0
<b>Data Processing</b>			
Labor	\$1,040	\$ 520	\$ 520
Software	\$ 100	\$ 0	\$ 100
Materials	\$ 40	\$ 40	\$ 0
<b>Data Presentation</b>			
Labor	\$ 130	\$ 130	\$ 0
Materials	\$ 10	\$ 10	\$ 0
<b>TOTAL</b>	<b>\$3,610</b>	<b>\$,2890</b>	<b>\$ 720</b>

The cost matrix above indicates an estimated increase in daily operating costs of \$720/day for the demonstrated EM63 technology over EM61 technology. This increase would be more than offset, however, if the EM63 was even partially successful at discriminating true UXO targets from clutter, thus reducing the number of UXO excavations. NAEVA has limited exposure to costs for UXO excavations, but a figure provided by ESTCP was \$200 per dig. Thus, eliminating just four digs per day would offset the additional costs of the demonstrated EM63 technology. In practice, if an “average” daily EM63 survey produced an average of 100 targets, and the demonstrated technology was able to eliminate *only 18%* of those targets from excavation, the cost savings would approximate the entire cost of conducting the digital geophysical mapping and discrimination. Higher levels of successful discrimination would yield potentially huge cost savings.

Specific to Kaho’olawe, the government reports, “As of 1 March 2000, contractors at Kaho’olawe had detected 12,121 subsurface anomalies and after digging they found that only 4 percent are UXO, 32 percent are false positives due to geologic variations and 64 percent are due

to buried metal from both UXO and non-UXO-related materials.” Using these figures, even if the demonstrated technology was able only to discriminate metal objects (both UXO and non-UXO) from magnetic rocks/soil, 32% of target excavations, more than 3,800 targets would have been eliminated with a savings of more than \$760,000 at a minimum (using the \$200 cost per dig figure from ESTCP).

Comparisons should also be made to mag-and-flag detection technology for which NAEVA does not have cost figures. Recent results from ESTCP’s JPG 2000 report indicate mag-and-flag detection percentages of only 65 to 70 percent, and a very high false alarm count. Thus, the demonstrated EM63 technology should have huge cost and performance advantages over mag-and-flag technology.

*This page left blank intentionally.*

## **6.0 IMPLEMENTATION ISSUES**

### **6.1 COST OBSERVATIONS**

Factors that affect project costs include, but are not limited to, the following:

- Project location
- Project size
- Terrain conditions
- Vegetation conditions
- Geologic terrain noise
- Scheduling requirements

#### **6.1.1 Project Location**

Project location affects mobilization and demobilization costs, and logistical support costs, such as shipment of spare parts, field crew break travel costs, and perhaps data transfer costs.

#### **6.1.2 Project Size**

Obviously, the larger the area to be surveyed, the longer it will take, and the more it will cost. Costs are not necessarily linear with acreage, however, as site-specific conditions within a project area may drastically affect costs per acre. Surveying 5 acres of difficult topographic terrain may be many times more costly than twice as much acreage of open flat terrain.

#### **6.1.3 Terrain Conditions**

Terrain conditions affect the speed at which a survey can precede and therefore how much ground can be covered per unit of time. A large area of flat open terrain could be surveyed with a vehicular towed-array system. Ground with moderate terrain conditions can be surveyed with a man-portable, wheel-mode cart system, while rugged terrain may have to be surveyed using a dual man portable “stretcher” configuration. Failure to implement the appropriate sensor transport configuration may compromise data quality. Surveying too fast may lengthen data point spacing beyond acceptable limits. Surveying in wheel-mode in rough terrain induces noise and “spikes” into the data. Sensor coils need to be kept parallel with and at a constant distance from the ground surface.

#### **6.1.4 Vegetation Conditions**

Surface vegetation conditions can have a major impact on project costs. Even moderately wooded terrain prohibits use of the EM63 instrument. Cleared woods allow use of the “stretcher” mode configuration, and open ground (fields) permits use of the man-portable or vehicular-towed configuration. Vegetation clearance can be very time-consuming and expensive, sometimes approaching or even exceeding the cost of the geophysical mapping.

### **6.1.5 Geologic Terrain Noise**

Geologic terrain noise is the influence of the bedrock (and/or overburden) on the background electromagnetic amplitude response. High geologic terrain noise complicates, or even prohibits, valid data interpretation of standard EM61 data. Using standard EM61 survey techniques in geologic noisy terrain causes a significant increase in false alarms and a decrease in successful percent detection. One of the great successes of our EM63 demonstration at Kaho'olawe was the ability to distinguish buried metal targets amidst very high geologic terrain conditions. Such ability would drastically reduce false alarms and therefore reduce costs. Generally, however, the lower the geologic terrain noise, the less complicated the data interpretation will be and the less costly the survey.

### **6.1.6 Scheduling Requirements**

Scheduling requirements can impact project costs. Rush jobs tend to have increased mobilization costs (higher shipping fees and travel costs). Sometimes a project (or client) requires very fast data processing turnaround time. This may necessitate implementation of an on-site processor, thus incurring higher costs for travel and living expenses.

### **6.1.7 Potential Cost Reductions/Cost Improvements**

The best approach to keeping costs low is through comprehensive advanced project planning. Adequate scheduling notice should be implemented to keep travel and shipping costs down. Presurvey site visits should be conducted to assess site-specific project conditions and objectives. Establishment of background geologic terrain noise should be accomplished during this visit. Consensus should be reached as to vegetation removal techniques that would optimize digital geophysical mapping. Historical research should be conducted to ascertain what ordnance types should be procured and made available to the contractor for measurement prior to initiation of field activities.

## **6.2 PERFORMANCE OBSERVATIONS**

Refer to Section 4.2 – Section 4.4.

## **6.3 SCALE-UP**

A concern in scale-up to a full-scale implementation would be equipment availability. The EM63 instrument, manufactured by Geonics Ltd. in Mississauga, Ontario, is not a mass-produced instrument. Only four or five have been manufactured to date, each one with significant modifications from previous versions. For full-scale implementation, sufficient notice should be given to the manufacturer to produce the number of instruments necessary to equip the project team(s). Every time sensor coil geometry and parameters are changed, detection/discrimination algorithms must be modified, and samples of inert ordnance items to be discriminated must be remeasured to reestablish the ordnance signature library for that ordnance suite. These issues may be mitigated in the future if the EM63 becomes used more commonly and its identity becomes standardized.

## **6.4 OTHER SIGNIFICANT OBSERVATIONS**

It is critical to correctly interpret the results of these demonstrations to properly evaluate the benefits and limitation of this discrimination technology.

## **6.5 LESSONS LEARNED**

Problems with instrument drift and instrument noise were limitations during the Kaho'olawe demonstrations. Geonics has been working on these problems, and reports (1) reduction in noise caused by a cooling fan in the instrument console and (2) software modifications for correction of early channel drift. This seems promising, but NAEVA-GPA cannot verify the degree of noise and drift reduction until new static tests are made. In future demonstrations or full-scale projects, additional time for testing and analysis of the EM63 will be required due to the continuing development by Geonics.

## **6.6 APPROACH TO REGULATORY COMPLIANCE AND ACCEPTANCE**

The primary regulatory issue, which will affect the adoption of discrimination technology such as EM63, will be gaining the confidence and approval of federal, state, and local regulators, stakeholders, and users. Acceptance by organizations such as the Army Corps of Engineers and Naval Facilities and Engineering Command will be needed in order that future RFPs will include such innovative technology. This controlled site ESTCP demonstration is the first to employ high magnetic (basaltic) conditions, which will allow side-by-side comparisons of discrimination performance, production rates, and costs. Acceptance of discrimination technology (that is, not digging some of a prioritized geophysical target list) ultimately requires a cost/risk evaluation by the regulatory agencies.

*This page left blank intentionally.*

## 7.0 REFERENCES

1. "The Parsons – UXB Express," Volume 2, Issue 3, 16 March 2000, Ref. 2.
2. McNeill, J.D. and Miro Bosnar, 1996, "Application of Time Domain Electromagnetic Techniques to UXO Detection," pp 34-42, Proceedings, 1996 UXO Forum.
3. Dabas, M., Jolivet, A., and Tabbagh, A., 1992, "Magnetic Susceptibility and Viscosity of Soils in a Weak Time Varying Field," *Geophys. J. Int.*, 108, pp 101-109.
4. Geonics Ltd, Jan. 2000, "EM63 Full Time Domain Electromagnetic UXO Detector, Operating Instructions."
5. Hien Dinh, NAVEODTECHDIV, Aug. 31, 2001, "Advanced UXO Detection/Discrimination Technology Demonstration, Kaho'olawe Island, Hawaii."
6. Technology Demonstration Plan - Advanced UXO Detection/Discrimination Technology Demonstration, Kaho'olawe, Hawaii. NAVEODTECHDIV, 20 August 2001.

*This page left blank intentionally.*

## APPENDIX A

### POINTS OF CONTACT

<b>Point of Contact (Name)</b>	<b>Organization (Name &amp; Address)</b>	<b>Phone/Fax/Email</b>	<b>Role In Project</b>
John Allan	NAEVA Geophysics Inc. P.O. Box 7325 Charlottesville, VA 22906	(434) 978-3187 (434) 973-9791 jallan@naevageophysics.com	Project Manager
G. Hunter Ware	Geophysical Associates P.O. Box 153 Ivy, VA 22945	(434) 293-6737 GHunterWare@aol.com	Principal Investigator



## **ESTCP Program Office**

**901 North Stuart Street  
Suite 303  
Arlington, Virginia 22203**

**(703) 696-2117 (Phone)  
(703) 696-2114 (Fax)**

**e-mail: [estcp@estcp.org](mailto:estcp@estcp.org)  
[www.estcp.org](http://www.estcp.org)**